

SYNTHESIS AND CHARACTERIZATION OF MESOGENIC SCHIFF
BASE ETHER,
P-N-(DIMETHYLAMINO)BENZYLIDENE-*P*-ALKYLOXYANILINES

By

KHOR KE XIN

KHOR KE XIN

B.Sc. (Hons.) Chemistry

2011

Faculty of Science,
Universiti Tunku Abdul Rahman,
In partial fulfillment of the requirements for the degree of
Bachelor of Science (Hons.) Chemistry
May, 2011

SYNTHESIS AND CHARACTERIZATION OF MESOGENIC SCHIFF
BASE ETHER,
P-N-(DIMETHYLAMINO)BENZYLIDENE-*P*-ALKYLOXYANILINES

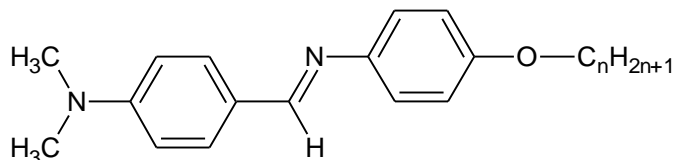
By

KHOR KE XIN

A project report submitted to the Department of Chemical Science,
Faculty of Science,
Universiti Tunku Abdul Rahman,
In partial fulfillment of the requirements for the degree of
Bachelor of Science (Hons.) Chemistry
May, 2011

ABSTRACT

A series of liquid crystal *p-n*-(Dimethylamino)benzylidene-*p*-alkyloxyanilines, **DBA-On** with different number of carbons at the terminal alkyl chain has been successfully synthesized.

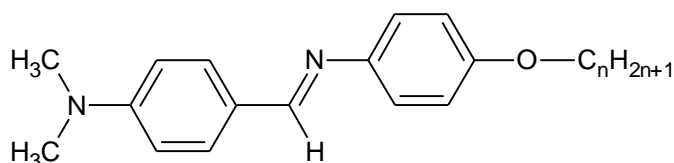


DBA-On, where $n = 6, 8, 10, 12, 14, 16$ and 18

The structure of the compounds is confirmed with the infrared (IR) spectroscopy, nuclear magnetic resonance (¹H and ¹³C NMR) spectroscopy and electron-ionization mass (EI-MS) spectrometry. The liquid crystal properties of these compounds were studied by using polarizing optical microscope (POM) attached to a Linkam hotstage and differential scanning calorimeter (DSC). In the series **DBA-On**, it can be concluded that **DBA-O6** to **DBA-O12** were identified as monotropic nematogens while **DBA-O14** to **DBA-O18** were non-mesogens. The structure-liquid crystal property relationship within the series and related structures reported in the literature was also studied.

ABSTRAK

Satu siri sebatian hablur cecair baru terbitan *p-n*- (Dimethylamino)benzylidene-*p*-alkyloxyanilines, **DBA-On** yang mempunyai bilangan karbon (n) yang berbeza dalam rantai alkil telah berjaya disintesis.



DBA-On, di mana $n = 6, 8, 10, 12, 14, 16$ dan 18

Struktur-struktur sebatian telah dikenalpasti dengan menggunakan kaedah spektroskopi inframerah (IR), resonans magnetik nukleus (^1H and ^{13}C NMR) dan spektrometrik jisim (EI-MS). Sifat hablur cecair telah dikaji dengan menggunakan mikroskop optikal berkutub (POM) yang disambungkan kepada pentas pemanasan Linkam dan kalorimeter pengimbasan perbezaan (DSC). Sebatian **DBA-O6** hingga **DBA-O12** telah dikenalpasti sebagai fasa nematik berdasarkan pemerhatian tekstur hablur cecair di bawah POM. Manakala, sebatian **DBA-O14** hingga **DBA-O18** telah diiktiraf sebagai sebatian yang tidak mempunyai sifat-sifat hablur cecair. Hubungan antara struktur kimia dan sifat hablur cecair dalam siri ini dan struktur berkaitan yang dilaporkan dalam literatur telah dikaji.

ACKNOWLEDGEMENTS

First of all, I want to give my deepest gratitude to Assistant Professor Dr. Ha Sie Tiong for his favour in this final year project. Discussions that he gave made my project proceeded in the right path. Guidelines, times and passion he gave to this project helped my project to be succeeded.

I would like to express my appreciation to Faculty of Science of Universiti Tunku Abdul Rahman for giving all the support in this final year project. I would like to thank the entire lab staffs for their help and assistant throughout the period of this project. I want to thank my teammate and fellow course mates that help me in this project.

I would like to thank Professor Dr. Yeap Guan Yeow (USM) and his post-graduate students for their collaboration in carrying out NMR analyses on some of my compounds. The great hospitality during the visit to his research laboratory for POM analyses was a great experience and I shall remember it.

I also want to mention my appreciation to National University of Singapore (NUS) for carrying out the EI-Mass Spectrometry for one of my compounds.

Eventually, I want give thankfulness to my family and aunties. Without their support, the project just would not be successful.

APPROVAL SHEET

I certify that, this project report entitled “ **SYNTHESIS AND CHARACTERIZATION OF MESOGENIC SCHIFF BASE ETHER, *P-N-(DIMETHYLAMINO)BENZYLIDENE-P-ALKYLOXYANILINES***”

was prepared by KHOR KE XIN and submitted in partial fulfillment of the requirements for the degree of Bachelor of Science (Hons.) in Chemistry at Universiti Tunku Abdul Rahman.

APPROVED by

Supervisor

Date: _____

(Dr. Ha Sie Tiong)

FACULTY OF SCIENCE
UNIVERSITI TUNKU ABDUL RAHMAN

Date: _____

PERMISSION SHEET

It is hereby certified that **KHOR KE XIN** (ID. No: **07ANB07423**) has completed this report entitled “**SYNTHESIS AND CHARACTERIZATION OF MESOGENIC SCHIFF BASE ETHER, P-N-(DIMETHYLAMINO) BENZYLIDENE-P-ALKYLOXYANILINES**” under supervision of **Dr. Ha Sie Tiong** from Department of Chemical Science, Faculty of Science.

I hereby give permission to my supervisors to write and prepare manuscript of these research findings for publishing in any form, if I did not prepare it within six (6) months time from this date provided that my name is included as one of the authors for this article. Arrangement of name depends on my supervisors.

DECLARATION

I hereby declare that project report is based on my original work except for quotations and citations which have been duly acknowledged. I also declare that it has not been previously or concurrently submitted for any other degree at UTAR or other institutions.

KHOR KE XIN

Date: _____

TABLE OF CONTENTS

	Page
ABSTRACT	i
ABSTRAK	ii
ACKNOWLEDGEMENTS	iii
APPROVAL SHEET	iv
PERMISSION SHEET	v
DECLARATION	vi
TABLE OF CONTENTS	vii
LIST OF TABLES	x
LIST OF FIGURES	xii
LIST OF ABBREVIATIONS	xiv

CHAPTER

1 INTRODUCTION	
1.1 Liquid Crystal	1
1.1.1 Historical of Liquid Crystal	2
1.1.2 Orientational and Positional Order	3
1.1.3 General Types of Liquid Crystal	5
1.1.3.1 Thermotropic Liquid Crystal	6
1.1.3.2 Mesogenic Materials	11
1.2 Objectives of the Project	13
2 LITERATURE REVIEW	
2.1 Liquid Crystals with Schiff Bases	14
2.2 Structure-Mesomorphic Properties Relationship	
2.2.1 Influence of Terminal Unit on Mesomorphic Properties	15
2.2.2 Influence of Linking Group on Mesomorphic Properties	18
2.2.3 Influence of Chain Length on Mesomorphic Properties	20
2.2.4 Influence of Lateral Group on on Mesomorphic Properties	22

3	MATERIALS AND METHODOLOGY	
3.1	Chemicals	27
3.2	Instruments	38
3.3	Synthesis	30
3.3.1	Synthesis of Synthesis of 4- {[4 (Dimethylamino)benzylidene]amino }phenol, DBAP	31
3.3.2	Synthesis of <i>p-n</i> -(Dimethylamino)benzylidene- <i>p</i> - alkyloxyanilines, DBA-On	31
3.3.2.1	Synthesis of <i>p-n</i> -(Dimethylamino)benzylidene- <i>p</i> - hexanoyloxyaniline, DBA-O6	31
3.3.2.2	Synthesis of <i>p-n</i> -(Dimethylamino)benzylidene- <i>p</i> - octanoyloxyaniline, DBA- O8	32
3.3.2.3	Synthesis of <i>p-n</i> -(Dimethylamino)benzylidene- <i>p</i> - decanoyloxyaniline, DBA- O10	32
3.3.2.4	Synthesis of <i>p-n</i> -(Dimethylamino)benzylidene- <i>p</i> - dodecanoyloxyaniline, DBA- O12	32
3.3.2.5	Synthesis of <i>p-n</i> -(Dimethylamino)benzylidene- <i>p</i> - tetradodecanoyloxyaniline, DBA- O14	33
3.3.2.6	Synthesis of <i>p-n</i> -(Dimethylamino)benzylidene- <i>p</i> - hexadecanoyloxyaniline, DBA- O16	33
3.3.2.7	Synthesis of <i>p-n</i> -(Dimethylamino)benzylidene- <i>p</i> - octadecaboyloxyaniline, DBA- O18	33
3.4	Characterization	
3.4.1	Infrared Spectral Analysis	34
3.4.2	Differential Scanning Calorimetry	34
3.4.3	Thin Layer Chromatography	35
3.4.4	¹ H and ¹³ C Nuclear Magnetic Resonance	35
3.4.5	Mass Spectroscopy Analysis	36
3.4.6	Liquid Crystal Texture and Transition Temperature Studies	36

4	RESULT AND DISCUSSION	
4.1	Synthesis and Characterization of 4-[(4-(Dimethylamino)benzylidene)amino]phenol	
4.1.1	Synthesis Route of 4-[(4-(Dimethylamino)benzylidene)amino]phenol, DBAP	37
4.1.2	Fourier Transform Infra-Red Analysis of DBAP	38
4.1.3	Mechanism of Imination	42
4.2	Synthesis and Characterization of <i>p-n</i> -(Dimethylamino)benzylidene- <i>p</i> -alkyloxyanilines, DBA-On	
4.2.1	Synthesis Route of Etherification	45
4.2.2	Infrared Spectrum Investigation on DBA-On	46
4.2.3	Mechanism of Williamson Etherification	52
4.2.4	Nuclear Magnetic Resonance	
4.2.4.1	¹ H NMR Spectrum Analysis	54
4.2.4.2	¹³ C NMR Spectrum Analysis	58
4.2.5	Mass Spectrometry Analysis	62
4.3	Mesomorphic Behaviour Analysis	
4.3.1	Polarizing Optical Microscope Analysis	67
4.3.2	Differential Scanning Calorimetry Thermogram Analysis	71
4.3.3	Influence of Structural Changes (Alkyl chain) on Temperature Changes of DBA-On	75
4.4	Structure Comparison with Related Compound	77
5	CONCLUSIONS	82
	REFERENCES	83

LIST OF TABLES

Table		
2.1	Structures, phase transition, transition temperature (°C) and enthalpies for compounds of series 3a-c and 5a-c , by Parra <i>et al.</i> (2004)	17
2.2	Structure, phase transition, transition temperature (°C) and enthalpies for compounds of series 6a-c , by Parra <i>et al.</i> (2004)	18
2.3	Structure, thermal stabilities (°C), of compounds 3 and compound A , by Prajapati <i>et al.</i> (2004)	19
2.4	Structure, transition temperatures (°C) and associated enthalpy changes of (kJ/mole) of nBABTH upon heating and cooling, by Ha <i>et al.</i> (2009)	22
2.5	Structure, transition temperature (°C) of 3-hydroxy-4-[(4-1, 2, 4-triazol-4-ylimino)methyl] phenyl 4-alkoxybenzoate of series A , by Thaker <i>et al.</i> (2009)	23
2.6	Structure, transition temperature (°C) of 3-hydroxy-4 (isonicotinoylcarbonohydrasonoyl) phenyl 4-alkoxybenzoate, by Thaker <i>et al.</i> (2009)	24
2.7	Structure, average thermal stabilities temperature (°C) of series 1, A, B, C , by Vora <i>et al.</i> (2002)	26
4.1	IR spectra data of 4-Aminophenol, 4-Dimethylaminobenzaldehyde and DBAP	41
4.2	IR spectra data of DBAP , Bromohexadecane and DBA-O16	49
4.3	IR spectra data of DBA-On , where n = 6, 8, 10, 12, 14, 16 and 18	51
4.4	¹ H NMR spectrum of <i>p-n</i> -(Dimethylamino)benzylidene- <i>p</i> -hexadecanoyloxyaniline, DBA-O16	57
4.5	¹³ C NMR spectrum of <i>p-n</i> -(Dimethylamino)benzylidene- <i>p</i> -hexadecanoyloxyaniline, DBA-O16	61
4.6	m/z value and the proposed fragment of DBA-O16	65

- 4.7 Transition temperatures of compounds **DBA-On**, n = 6, 8,10, 12, 14, 16 and 18, upon heating and cooling, obtained from DSC 74
- 4.8 Comparison of liquid crystalline properties of **DBA-O12** with **A**, Han *et al.* (2004) and **Series 1**, Vora *et al.* (2000) 78

LIST OF FIGURES

Figure		
1.1	Schematic illustration of the solid, liquid crystal, and liquid phases	2
1.2	Structure of cholesteryl benzoate with two melting points	3
1.3	Schematic arrangement of molecules in various phases	4
1.4	Classification of phases of liquid crystal	5
1.5	Molecular structure of (a)cholesteryl benzoate Molecular structure of (b) <i>p</i> -azoxyanisole Molecular structure of (c)triphenylene	6
1.6	Molecular arrangement and texture of nematic liquid crystal	7
1.7	Molecular arrangement and texture of cholesterics phase liquid crystal	8
1.8	Molecular arrangement and texture of (a)SmA phase Molecular arrangement and texture of (b)SmC phase Molecular arrangement and texture of (c)SmC* phase	11
1.8	Typical calamitic liquid crystal	12
2.1	Structure of 4-hexyloxybenzylidene-4'-alkyloxyanilines, by (Godzwon <i>et al.</i> , 2007)	15
2.2	Plot of transition temperatures versus the number of carbons (n) in the alkanoyloxy chain of nBATH during heating cycle, n=2, 3,4, 5, 6, 8, 10, 12, 14, 16 and 18 by Ha <i>et al.</i> (2009)	21
3.1	Reaction scheme for preparing DBAP and final product, DBA-On	30
4.1	Synthesis route of Schiff base formation, DBAP	37
4.2	IR spectra of 4-Dimethylaminobenzaldehyde, 4-Aminophenol and DBAP	40
4.3	Mechanism of imination	44

4.4	Etherification route between DBAP and various length of bromoalkanes	45
4.5	IR spectra of DBAP , Bromohexane and DBA-O16	48
4.6	IR Spectra of DBA-On , n= 6, 8, 10, 12, 14, 16 and 18	50
4.7	Mechanism of the Williamson Etherification	53
4.8	¹ H NMR spectrum of <i>p-n</i> -(Dimethylamino)benzylidene- <i>p</i> -hexadecanoyloxyaniline, DBA-O16	56
4.9	¹³ C NMR spectrum of <i>p-n</i> -(Dimethylamino)benzylidene- <i>p</i> -hexadecanoyloxyaniline, DBA-O16	60
4.10	EI-Mass spectrum of <i>p-n</i> -(Dimethylamino)benzylidene- <i>p</i> -hexadecanoyloxyaniline, DBA-O16	66
4.11a	Optical photomicrograph of DBA-O12 undergoes phase transition of isotropic to nematic during its cooling cycle	69
4.11b	Optical photomicrograph of DBA-O12 exhibiting nematic droplets texture and homeotropic texture during its cooling cycle	69
4.12	Optical photomicrograph of DBA-O6 exhibiting nematic droplets texture and homeotropic texture during its cooling cycle	70
4.13	DSC thermogram for DBA-O12	73
4.14	Plot of phase transition temperatures against number of carbon atom (n) in alkyloxychain chain during heating scan	76

LIST OF ABBREVIATIONS

DBA-O6	<i>p-n</i> -(Dimethylamino)benzylidene- <i>p</i> -hexanoyloxyaniline
DBA-O8	<i>p-n</i> -(Dimethylamino)benzylidene- <i>p</i> -octanoyloxyaniline
DBA-O10	<i>p-n</i> -(Dimethylamino)benzylidene- <i>p</i> -decanoyloxyaniline
DBA-O12	<i>p-n</i> -(Dimethylamino)benzylidene- <i>p</i> -dodecanoyloxyaniline
DBA-O14	<i>p-n</i> -(Dimethylamino)benzylidene- <i>p</i> -tetradecanoyloxyaniline
DBA-O16	<i>p-n</i> -(Dimethylamino)benzylidene- <i>p</i> -hexadecanoyloxyaniline
DBA-O18	<i>p-n</i> -(Dimethylamino)benzylidene- <i>p</i> -octadecanoyloxyaniline
DBAP	4-{[4(Dimethylamino)benzylidene]amino}phenol
EtOH	Ethanol
KOH	Potassium hydroxide
DSC	Differential Scanning Calorimetry
FTIR	Fourier Transform Infrared
LC	Liquid Crystal
N	Nematic
NMR	Nuclear Magnetic Resonance
POM	Polarising Optical Microscope
ppm	Parts per million
SmA	Smectic A
SmC	Smectic C
TMS	Tetramethylsilane

CHAPTER 1

INTRODUCTION

1.1 Liquid Crystal

The term liquid crystal signifies a state of aggregation that is intermediate between the crystalline solid and the amorphous liquid as shown in Figure 1.1 (Chandrasekhar, 1992). A substance in this state flows like liquids, yet possesses some physical properties characteristic of crystals. Materials that exhibit such unusual phase are known as mesogens, and the various phases in which they could exist are called mesophases. The occurrence of mesomorphism entails a crucial requirement which is the molecule must be highly geometrically anisotropic in shape, like a rod or disc (Chandrasekhar 1992). By transforming a system into the isotropic liquid, the system may pass through one or more mesophases before the transformation which depend on the detailed molecular structure. Transitions to these intermediate states may be brought about by purely thermal processes (thermotropic mesomorphism) or by the influence of solvent (lyotropic mesomorphism). As a function of temperature, or depending on the constituents, concentration, substituent, and so on, the existence of liquid crystal in many mesophases include nematic, cholesteric, smectic (Lam, 2007).

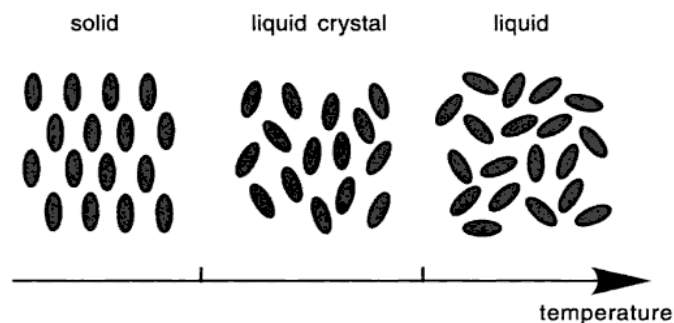


Figure 1.1: Schematic illustration of the solid, liquid crystal, and liquid phases. The elliptical shapes represent molecules

1.1.1 History of Liquid Crystal

The liquid crystalline state was detected more than 100 years ago. The study of liquid crystal is begun in 1888, an Austrian botanist named Friedrich Reinitzer had reported on the colored phenomena occurring in melts of compounds known as cholesteryl benzoate and cholesteryl acetate which are natural products occurring in plants and animals. Reinitzer found these esters of cholesterol have two distinct melting points which are 145.5 and 178.5 °C (Fisch, 2006). In the case of cholesteryl benzoate, at 145.5 °C, the crystal transformed to a cloudy fluid and turned into a clear liquid at 178.5 °C. In addition, some unusual colour behavior was also observed upon cooling. Firstly, the appearance of pale blue was observed when the clear liquid turned cloudy. Then, a bright blue-violet colour was observed as the crystal crystallized (Singh, 2001). Otto Lehmann, German Physicists who was studying the crystallization properties of various substances, studied the samples from Reinitzer through his polarising microscope.

He found that the materials flow like liquid and exhibit optical behaviour like that of the crystal. Lehmann then named them as liquid crystal after he assured that the opaque phase was a uniform phase of matter sharing properties of both liquids and solids. Figure 1.2 shows the structure of cholesteryl benzoate with two distinct melting points.

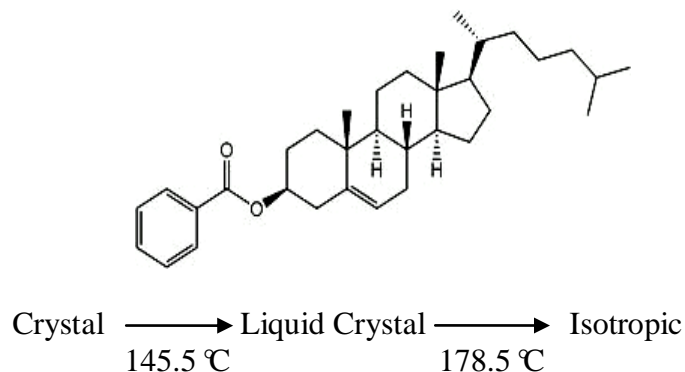


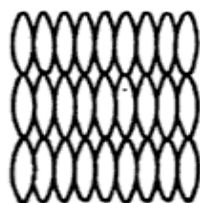
Figure 1.2: Structure of cholesteryl benzoate with two melting points

1.1.2 Orientational and Positional Order

Various liquid crystal phases can be characterized by the type of ordering. Typically, a crystal consists of molecules arranged in ordered form while in liquid they are not. The existing order of in a crystal is usually both positional and orientational (Singh, 2001). Following possibilities may exist when a molecule material composed of anisotropic materials is heated from the solid phase at the melting point.

- a. The phase will be an “isotropic liquid” possessing a $T(3) \times O(3)$ symmetry if both order positional and orientational disappear concurrently.

- b. The phase known as “plastic crystal” as the positional order intact and absent of the orientational order. Materials possess this rotator phase have their molecules rotate freely along one or more of their molecular axes while their center of mass are fixed in a lattice.
- c. The phase with fully or partially disappearance of positional order and some degree of orientational order is retained is called “liquid crystal” , mesophase or mesomorphic phase. The unique axes of the molecules in this phase are remained, on average, parallel to each other, leading to a preferred direction in space. A compound possess a mesophase is called mesogenic compound.
- d. The arrangement of molecules is regular, with a regularly repeating pattern in all directions. The molecules are held in fixed positions by intermolecular forces. This phase is known as “crystalline solid” state.



Crystalline solid



Isotropic liquid



Plastic crystal



Liquid crystal

Figure 1.3: Schematic arrangement of molecules in various phases

1.1.3 General types of Liquid Crystal

Liquid crystalline materials are classified into two categories which are thermotropic and lyotropic mesophases as shown in Figure 1.4 (Dierking, 2003). Thermotropic liquid crystals phases can be observed via the change of temperature while the appearance of lyotropic phases affected by the presence of suitable (isotropic) solvent. Amphotropic are name for those mesogen which able to form both lyotropic and thermotropic mesophases. Thermotropic liquid crystals are further classified to three basic molecular shapes which are called calamitic for rod-like, discotic for disk-like and sanidic for brick- or lath-like molecules. Calamitic mesogens are rigid cores, often incorporating phenyl and biphenyl groups, and two flexible endgroup which are mostly alkyl or alkoxy chains (Dierking, 2003). While for discotic mesogens, six flexible endgroups are attached to a rigid, disc-like core.

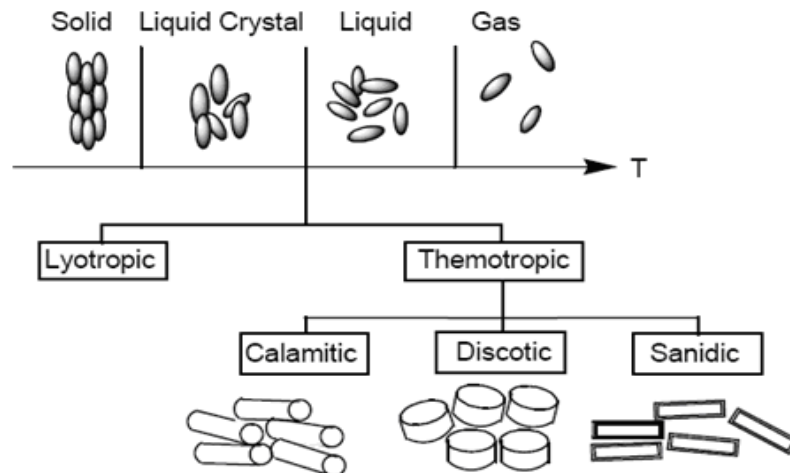
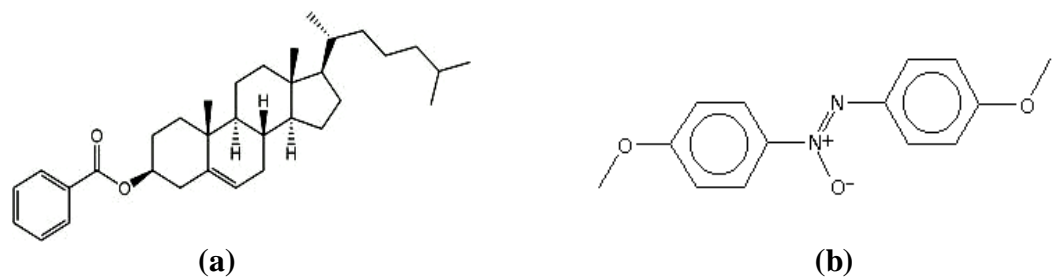


Figure 1.4: Classification of phases of liquid crystal

Example of calamitic mesogens:



Example of discotic mesogens:

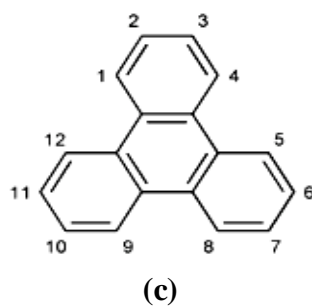


Figure 1.5: Molecular structure of (a)cholesteryl benzoate (b) *p*-azoxyanisole (c)triphenylene

1.1.3.1 Thermotropic Liquid Crystals

The phases of thermotropic liquid crystals can be classified into three main phases which are nematic, cholesteric and smectic.

a. Nematic phase

The nematic liquid crystal is the one with the least order and highest symmetry with the most liquid-like structure in which one or two molecular axes are oriented parallel to one another, resulting in an orientational long range order. For instance, an angular distribution of the long molecular axis around a particular direction, the director n , while the molecules' centres of mass are isotropically distributed in all three dimensions (Dierking, 2003). The director n is the average local direction of long molecular axis and represents the direction of the optic axis of the system. The preferred direction usually varies from point to point in the medium, but a uniformly aligned specimen is optically uniaxial, positive and strongly birefringent. The nematic liquid crystals exhibit marble like texture under observation of POM as shown in Figure 1.6.

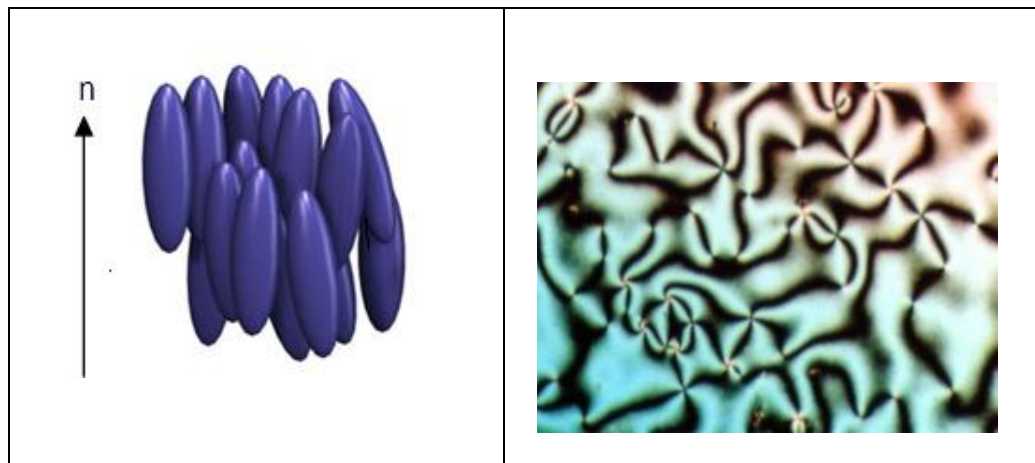


Figure 1.6: Molecular arrangement and texture of nematic liquid crystal

b. Cholesterics phase

The cholesterics phase often known as the chiral nematic liquid crystal which tends to align in a helical manner. This property results from synthesis of cholesteric liquid crystal. It is obtained through addition of chiral molecules to a nematic liquid crystal. Some materials such as cholesterol ester are naturally chiral. The phase occurs as a slowly twisted nematic phase which is rod-shaped and in layered structure (Collings, 2002). A fingerprint texture can be seen under the observation of POM as shown in Figure 1.7.

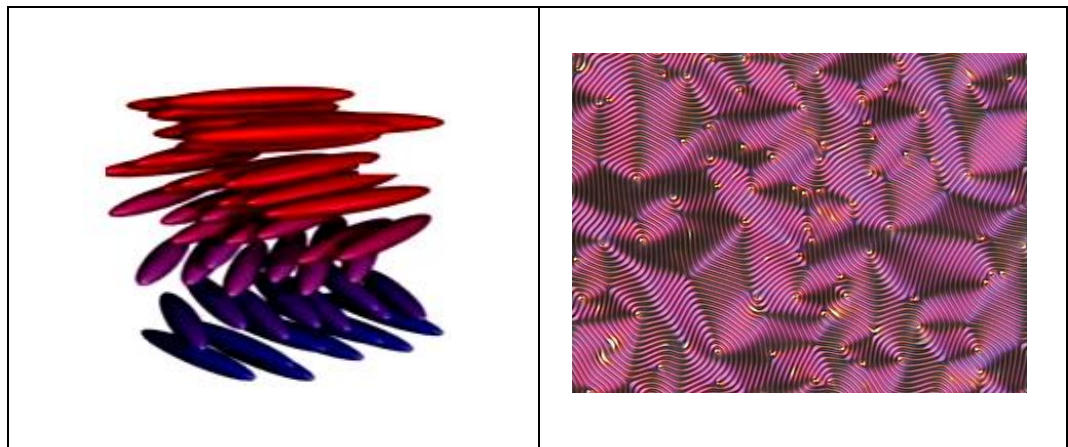


Figure 1.7: Molecular arrangement and texture of cholesterics phase liquid crystal

c. Smectic phase

Smectic liquid crystal possesses positional order which mean the position of the molecules is correlated in some ordered pattern. The occurrence of the phase is usually at the temperature below the nematic phase. The term “smectic” is came from the Greek word “soap”. There are many types of smectic phases which are smectic A, smectic C, smectic C*(ferroelectrics). In each layered structure of a smectic A liquid crystal, the molecules are in random position, but directionally ordered with their long axis normal to the plane of the layer (Collings, 2002). Under the observation of POM, it exhibits focal-conic texture as shown in Figure 1.8a.

The molecules of smectic C liquid crystal are in random position within each layer. Formation of smectic C phase require molecules that are either non-chiral or form a racemic mixture. The structure of smectic C is broken-fan shape under observation of POM as shown in Figure 1.8b. As in the nematic, the smectic C mesophase has a chiral state designated C* in smectic C*, the direction of molecules varies continuously from layer to layer forming a helix as shown in Figure 1.8c.

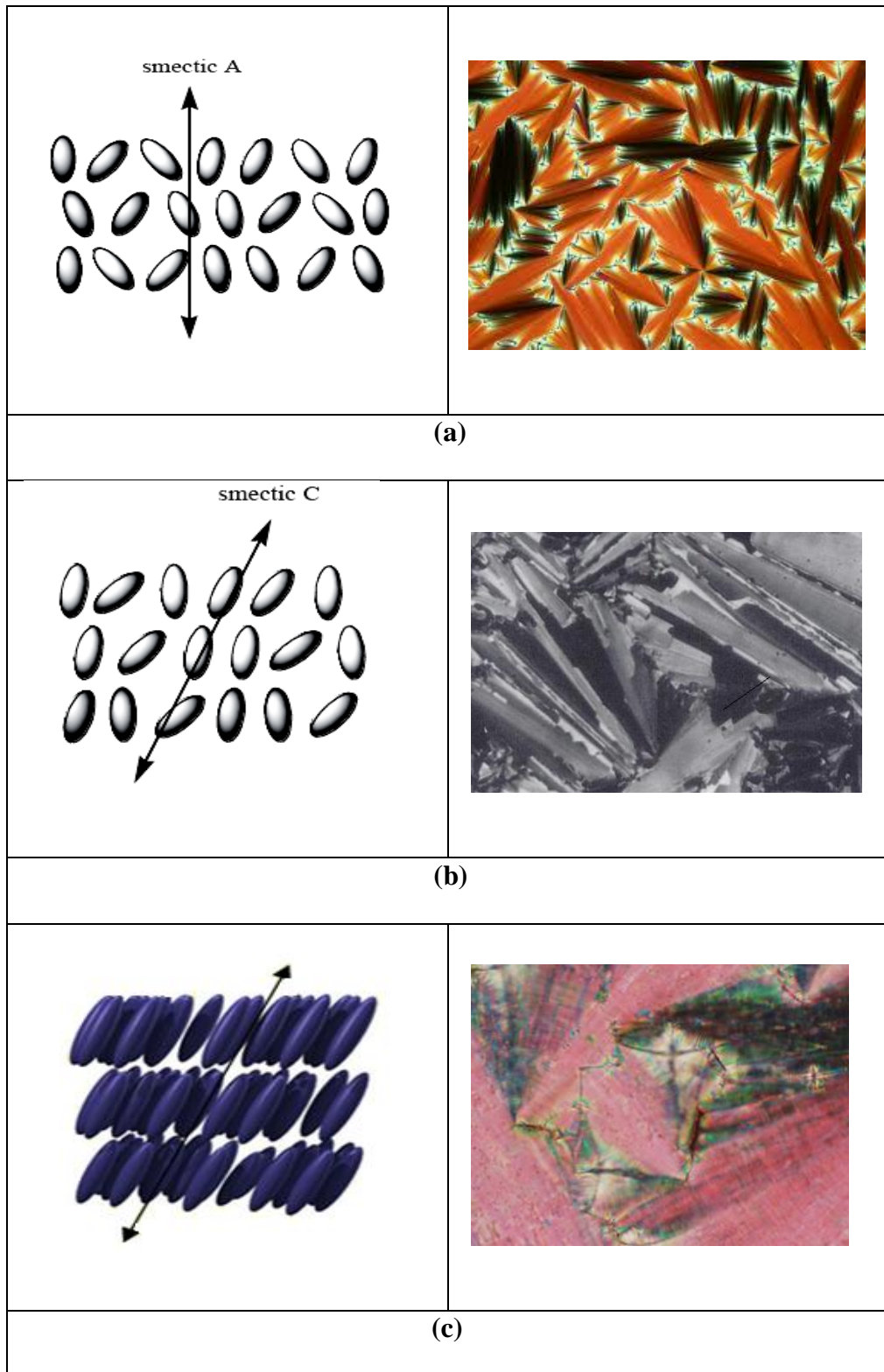


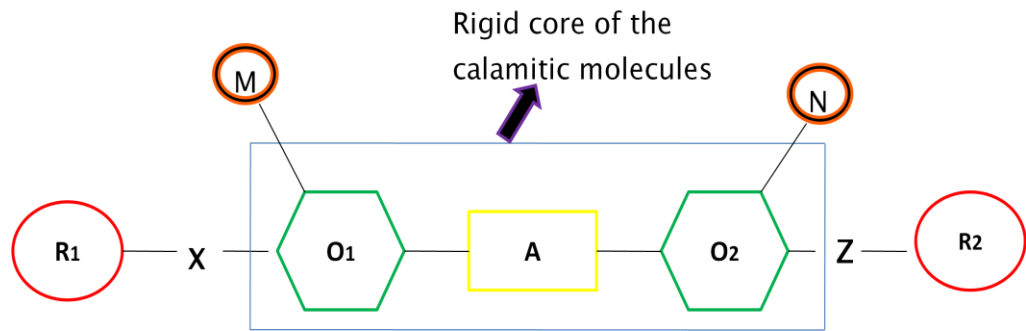
Figure 1.8: Molecular arrangement and texture of (a)SmA phase (b)SmC

phase (c)SmC* phase

1.1.3.2 Mesogenic Materials

Each different structural class of material may illustrate different types of liquid crystalline phases. The mesogenic molecules must be either in elongated or disc-like shape. As shown in Figure 1.9, the rigid core of the calamitic molecules is formed by the bridging group A together with the ring structures O₁, O₂. Schiff bases, diazo and azoxy compounds, nitrones, esters and etc. are usually used as the bridging group while aromatic rings are usually opt for ring structures. The core rigidity of the molecules which typically provided by linearly ring system (O₁, O₂) is crucial in forming a liquid crystalline phase as it creates the interactions with other molecules anisotropic. Normally, both terminal groups R₁ and R₂ can be linked directly to the core or through groups X and Z.

The liquid crystal phases might not formed by relying on the rigid core alone. Thus, certain flexibility is required to ensure reasonably low melting points and to stabilise the molecular alignment within the mesophase structure (Singh, 2002). Terminal substituents R₁ and R₂ which may be polar (e.g., CH₃) or nonpolar (e.g., CN, F) usually provide the flexibility. M and N are the lateral substituents which involved in the modification of phase morphology and the physical properties of materials.



R1 and R2 : Terminal substituent (e.g CH₃, CN, F etc.)

O1 and O2 : Ring structure

X,A and Z : Linking group (e.g ester, imine)

M and N : Lateral substituent (e.g hydroxy, halogen)

Figure 1.9: Typical calamitic liquid crystal

1.2 Objective of the Project

The objectives of the project are:

1. To synthesis *p-n*-(Dimethylamino)benzylidene-*p*-alkyloxyanilines, **DBA-On**, n= 6, 8, 10, 12, 14, 16 and 18.
2. To characterize the structure of *p-n*-(Dimethylamino)benzylidene-*p*-alkyloxyanilines, **DBA-On** by using FT-IR, NMR and Mass Spectroscopic technique, n= 6, 8, 10, 12, 14, 16 and 18.
3. To determine liquid crystal properties of *p-n*-(Dimethylamino)benzylidene-*p*-alkyloxyanilines, **DBA-On** by using DSC and POM n= 6, 8, 10, 12, 14, 16 and 18.

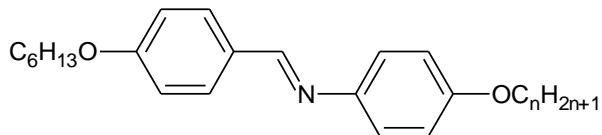
CHAPTER 2

LITERATURE REVIEW

2.1. Liquid Crystals with Schiff Bases

Nowadays, thermotropic liquid crystals have become important materials in the world of liquid crystal science and technology. Schiff bases are being recognized since 1970 after the publication of Kelker about methoxybenzylidene-butylaniline (MBBA). The discovery of MBBA which exhibits a nematic phase at the room temperature is a starting point for studies relating to the liquid crystalline behavior of the Schiff bases. Schiff base, also known as imine ($\text{CH}=\text{N}$), possesses a useful functional group due to its rich polymorphism and convenience by its low temperature of phase transition.

Imine is an essential linking group used in connecting two core groups. It is able to maintain molecular linearity although it provides a stepped core structure. Thus, it enhances the stability and induces the formation of the mesophase. Godzwon *et al.* (2007) has reported on a homologous series of 4-hexyloxybenzylidene-4'-alkyloxyanilines nematic, smectic A, smectic C, smectic I and smectic F mesophases.



Where $n = 1, 2, 3, 4, 5, 6, 7, 8, 9, 10, 11, 12$

Figure 2.1: Structure of 4-hexyloxybenzylidene-4'-alkyloxyanilines, by (Godzwon *et al.*, 2007)

2.2 Structure- Mesomorphic Properties Relationship

2.2.1 Influence of Terminal Unit on Mesomorphic Properties

Chain branching shows an apparently effect on the mesomorphic phase behaviour as it helps in introducing chirality into a molecule. However, the melting point and phase stability are being reduced as a result of the disruption in the molecular packing (Singh, 2002). In addition, the position of end chains influences the formation of mesophase as well.

Two new homologous series of Schiff's bases containing the 1, 3, 4-thiadiazole ring namely series **3a-c** and series **5a-c** respectively has been reported by Parra *et al.* (2004). Each of the compounds possesses different terminal substituent and liquid crystalline properties in which one substituent is a terminal alkoxy group with the number of carbon atoms kept at $n=10$ while the other terminal substituent is an flexible ester chain.

All compounds in the series **3a-c** displayed mesomorphic properties, an enantiotropic smectic A mesophase can therefore be observed. The enantiotropic

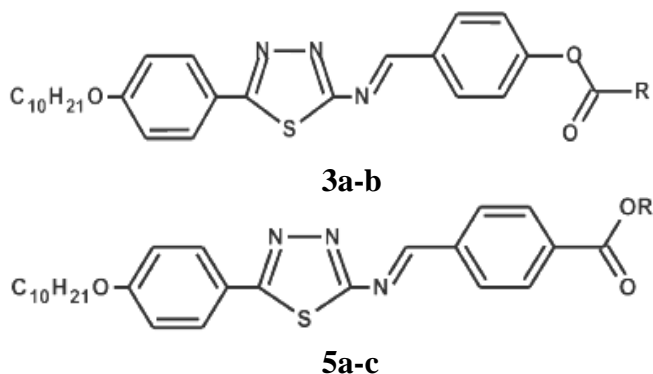
nematic phase of series **5a-c** shows an odd-even alternation effect for the crystal to nematic and nematic to isotropic transition. From Table 2.1, compounds of series **3** and **5** have a higher melting point and a lower clearing temperature than the compound of series **5a-c**. The dissimilarity between series **3a-c** and **5a-c** is in their lateral ester chain which possessed by each of the series. The result shows that the position of the carbonyl group has an intense influence on the mesogenic properties.

From the mesophase displayed by both series, it is obvious that the smectic A phase is more favoured for the carbonyl group connected away from the aromatic rigid core. This information indicates that the lateral dipolar interactions associated with terminal ester chain dipoles dominate phase structure in smectic liquid crystals (Parra *et al.*, 2004).

The mesomorphic properties of the Schiff's bases of series **3a-c** and series **5a-c** is compared with Schiff's bases of series **6a-f**. The compounds of series **6** possess a similar central rigid core as those of the series **3** and **5** but different in their lateral flexible chains. The former have an alkoxy chain and an ester chain at the end of the rigid core, whereas the latter have two lateral alkoxy chains. The compounds of series **6** displayed smectic C and nematic (N) mesomorphism instead of smectic A meosphase in the whole range of n studied. The melting points of imines in series **6** are lower and have broader mesomorphic ranges which is approximately 90 °C than the imines of series **3** and **5**.

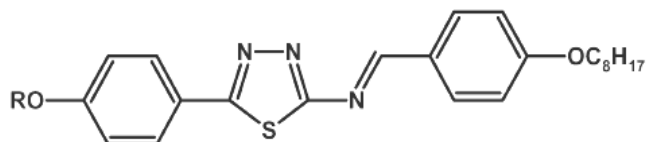
Probably, a lateral interaction giving rise to a layered smectic order is more favoured for the compounds of series **3** and **6** as compared with their analogues in series **6**. This is due to the best packing molecular arrangement which has an effect on the strength of the dipolar interactions (Parra *et al.*, 2004).

Table 2.1: Structures, phase transition, transition temperature (°C) and enthalpies for compounds of series 3a-c and 5a-c, by Parra *et al.* (2004)



Compound, R=n- C _n H _{2n+1}	Transition	Temperature (°C)	ΔH/kJ mol ⁻¹
3b (n=8)	Cr-SmA	140.2	12.5
	SmA-I	151.7	7.7
3c (n=9)	Cr-SmA	117.7	8.3
	SmA-I	157.6	8.0
5a (n=8)	Cr-N	118.1	27.5
	N-I	175.7	4.1
5a (n=9)	Cr-N	107.1	17.3
	N-I	170.1	2.9

Table 2.2: Structure, phase transition, transition temperature (°C) and enthalpies for compounds of series 6a-c, by Parra *et al.* (2004)



Compound, R= n-C _n H _{2n+1}	Transition temperature (°C)	
6d (n=8)	Cr-SmC	107.8
	SmC-N	193.9
	N-I	205.2
6e (n=9)	Cr-SmC	106.8
	SmC-N	193.5
	N-I	201.1

2.2.2 Influence of Linking Group on Mesomorphic Properties

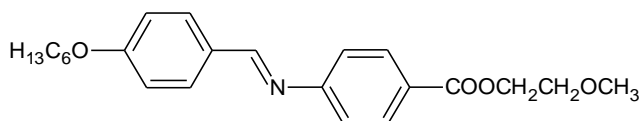
One of the useful methods for reducing the transition temperature and destabilizing the mesophase is the use of bridging group as it commences flexibility in the material.

The effect of a Schiff's base linkage on mesomorphism has been discussed by Prajapati *et al.* (2004). Compound **3** has higher smectic mesophase range and smectic mesophase thermal stability than compound **A** by 6 °C and 34 °C as shown in Table 2.3. Two different central linkages can be found in compound **3** and compound **A**. Compound **3** has an azomethine (-CH=N-) central linkage whereas compound **A** has an ester (-COO-) central linkage. The azomethine

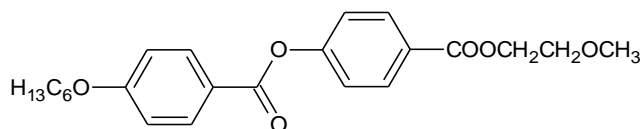
central linkage is more coplanar than the ester (-COO-) central linkage and allows the molecules to pack more efficiently. Thus, the smectic thermal stability of compound **3** is higher than compound **A**.

Besides, it is also known that the liquid-crystalline properties are enhanced most when all the rings are conjugated. For instance, a high liquid crystal transition temperatures can be achieved when the entire system is linked through central linking groups involving multiple bonds such as -CH=N- or -CH=CH- (Prajapati *et al.*, 2004) . However, the central ester linkage does not link the system through a multiple bond. Hence the mesogenic thermal stability of a system connected via an azomethine linkage is higher.

Table 2.3: Structure, thermal stabilities (°C), of compounds **3 and compound **A**, by Prajapati *et al.* (2004)**



Compound 3



Compound A

Compound number	Thermal stabilities (°C)	
	Sm	N
3	77	-
A	43	-

2.23 Influence of Chain Length on Mesomorphic Properties

The use of a fairly long and hydrocarbon chain which is usually alkyl or alkoxy has become one of the most successful route in the formation of liquid crystals. Often, the role of this group is to act as either a flexible extension to the core or as a dipolar moiety to introduce anisotropy in physical properties.

In the series of Schiff's base esters with benzothiazole and aromatic cores, 2-(4-alkanoyloxybenzylidenamino)benzothiazoles, **nBABTH**, Ha *et al.* (2009) stated that the short derivatives where $n = 2, 3, 4, 5, 6, 8$, are non-mesogens. The mesophase starts to emerge as a monotropic (metastable) smectic A phase beginning with the *n*-decanoyloxy derivative. The commencement of enantiotropic (stable) smectic A phase is observed when the length of the carbon chain increases from the *n*-dodecanoyloxy to the *n*-hexadecanoyloxy derivative. The increase of smectic A phase range can be observed from **12BABTH** (4.8 °C) to **14BABTH** (8.4 °C) and then decreased for **16BABTH** (5.0 °C). The smectic phase for **18BABTH** turns to a monotropic phase upon further increasing the length of the carbon chain. This information indicates the flexibility provided by the carbon chain has significant impact on the mesophase.

In general, high rigidity of molecules perturb the generation of liquid crystals phase. As the length of terminal chain is increased, the molecule becomes more flexible therefore promoting a monotropic mesophase in a particular

compound (Ha *et al.*, 2009). An enantiotropic mesophase may be formed as increases the length of carbon chain continually. However, the depression of stability of mesophase will be induced as the length of chain keeps increasing.

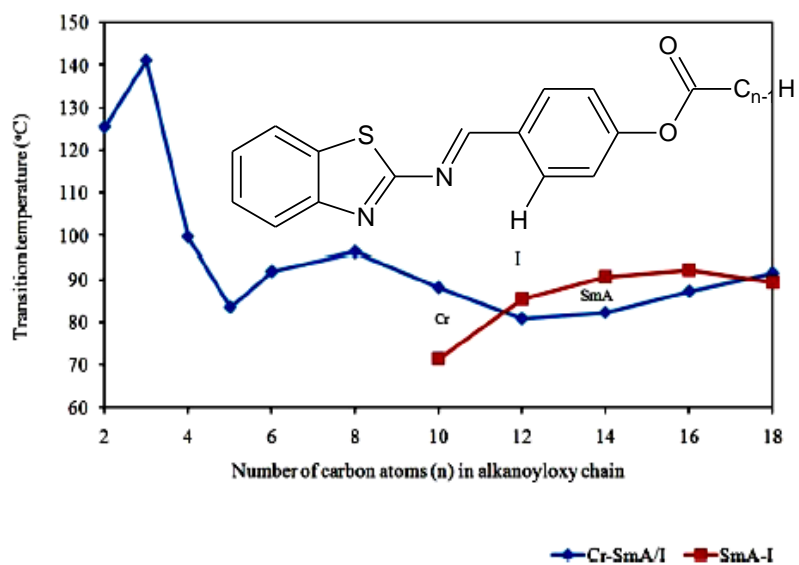
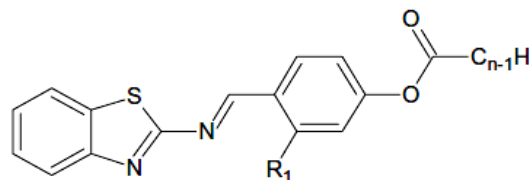


Figure 2.2: Plot of transition temperatures versus the number of carbons (n) in the alkanoyloxy chain of nBABTH during heating cycle, n=2, 3, 4, 5, 6, 8, 10, 12, 14, 16 and 18 by Ha *et al.* (2009)

Table 2.4: Structure, transition temperatures (°C) and associated enthalpy changes of (kJ/mole) of nBABTH upon heating and cooling, by Ha *et al.* (2009)



$R_1 = H$ where $n = 2, 3, 4, 5, 6, 8, 10, 12, 14, 16, 18$

Compound	Transition temperatures, °C (ΔH , kJmol ⁻¹)
2BABTH	Cr 125.5 (31.82) I
8BABTH	Cr 94.2 (7.74) I Cr 82.3 (7.26) I
16BABTH	Cr ₁ 64.9 (2.21) Cr ₂ 79.5 (2.61) Cr ₃ 87.3 (44.24) SmA 92.3 (8.73) I Cr ₁ 57.3 (3.71) Cr ₂ 67.8 (44.72) SmA 89.1 (9.79) I
18BABTH	Cr ₁ 69.6 (3.44) Cr ₂ 91.5 (64.29) I Cr ₁ 63.7 (3.84) Cr ₂ 75.6 (48.69) SmA 89.4 (10.41) I

2.24 Influence of Lateral Group on Mesomorphic Properties

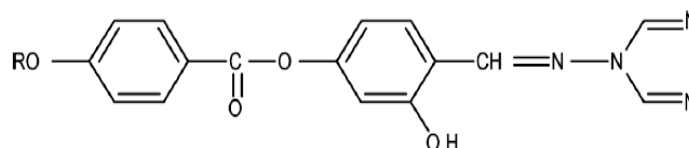
Two new mesogenic homologous series of liquid crystalline compound containing 1,2,4-triazole and isonicotinic acid ring at the terminus of the molecule have been reported by Thaker *et al.* (2009), namely 3-hydroxy-4-[(4-1,2,4-triazol-4-ylimino)methyl] phenyl 4-alkoxybenzoate (Series A) and 3-hydroxy-4-(isonicotinoyl carbonohydrazonoyl) phenyl 4-alkoxy benzoate (Series B).

The molecular ordering can be enhanced with the presence of lateral hydroxyl group which then leads to higher clearing temperature. By comparing two series, it is observed that the clearing temperature of compounds of series A

are considerably higher than compounds of series **B**. This indicates that the introduction of hydroxyl group at the ortho position in the aldehyde fragment increases the degree of anisotropy of the molecular polarizability of compounds in both the series. Therefore, the degree of molecular order can be increased, causing the stability of smectic phase to increase.

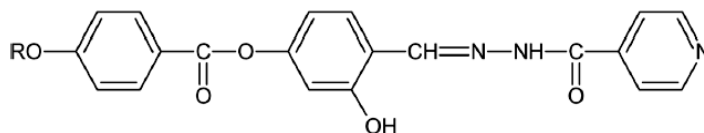
By studying the transition temperature of both series, the introduction of hydroxy group at the ortho position in the aldehyde fragment triggers the degree of anisotropy of the molecular polarizability of compounds of both series to increase. This increases the van der waals forces and therefore contributes to high degree of stability on mesophase.

Table 2.5: Structure, transition temperature (°C) of 3-hydroxy-4-[(4-1, 2, 4-triazol-4-ylimino)methyl] phenyl 4-alkoxybenzoate of series A, by Thaker *et al.* (2009)



Compounds	Transition Temperature (°C)			
	R= n alkoxy	SmC	N	I
A₁₀	Decyl	-	147	188
A₁₂	Dodecyl	109	141.14	173
A₁₄	Tetradecyl	86	132	160
A₁₆	Hexadecyl	72	124.92	146

Table 2.6: Structure, transition temperature (°C) of 3-hydroxy-4 (isonicotinoylcarbonohydrazonoyl) phenyl 4-alkoxybenzoate, by Thaker *et al.* (2009)



Compounds	R= n alkoxy	Transition temperature (°C)		
		Sm	N	I
B₁₀	Decyl	99 (SmC A)	139	183.59
B₁₂	Dodecyl	85	102	180
B₁₄	Tetradecyl	77 (SmC A)	83	178.01
B₁₆	Hexadecyl	62	70	162

Four mesogenic homologous series containing three rings in the main core and substituted by a lateral acetyloxy group or hydroxy group on the central benzene nucleus has been studied though Vora *et al.* (2002).

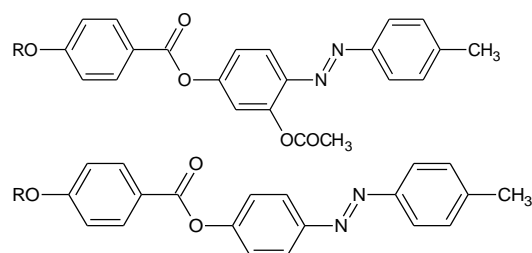
Based on Table 2.7, series **1** has lower average nematic stabilities as compare with those of series **A**. The molecules of series **1** have increase breadth due to the lateral acetyloxy (CH₃COO-) group on the central benzene ring. The low average nematic thermal stability of series **1** probably cause by the depression of lateral substituents on thermal stabilities of the compounds.

Series **1** which has lateral acetyloxy group has higher average nematic thermal stability than series **B** which possess a hydroxy group at that position. Due to the intramolecular association of lateral hydroxyl group with an azo central linkage it is less effective in broadening of the molecules of series **B**

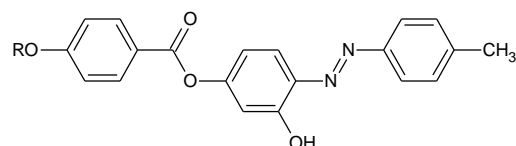
whereas the effect of increase in the breadth is prominent in series **1** because of the lateral acetyloxy group (Vora *et al.*, 2002). Thus, the average nematic thermal stability of series **1** is low.

Each series **C** and series **1** displayed smectic C mesophase and nematic mesophase respectively. The molecules of series **C** are arranged in the lamellar sheets which are characterized by a parallel molecular alignment with an interlocking of neighbouring molecules by their bulky branches and intercalation of the alkyl chain (Vora *et al.*, 2002). But, the lateral motif in the series **1** induces the formation of nematic phase, preventing the more ordered in plane molecular association needed for smectic arrangement as observed in the number of homologous series. Therefore, series **1** exhibits only nematic phase. In short, the short aliphatic chain can stabilize the nematic phase whereas long aromatic lateral substituents stabilize smectic phase.

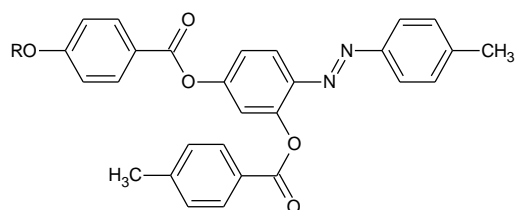
Table 2.7: Structure, average thermal stabilities temperature (°C) of series 1, A, B, C, by Vora *et al.* (2002)



Series 1



Series B



Series A

Series C

Series	SmC-/ N-I (C ₄ - C ₈)	Commencement of smectic phase
1	101.2	-
A	227.8	-
B	233.0	-
C	39.2	C ₄

CHAPTER 3

MATERIALS AND METHODOLOGY

3.1 Chemical

The chemical used in the project are listed as following:

1. Chemical obtained from Merck, Germany:
 - a. 1-Bromohexane
 - b. 1-Bromooctane
 - c. 1-Bromodecane
 - d. 1-Bromododecane
 - e. 1-Bromotetradecane
 - f. 1-Bromohexadecane
 - g. 1-Bromooctadecane
 - h. 4-Aminophenol
 - i. Potassium hydroxide
 - j. Acetic acid
 - k. TLC plates

2. Chemical obtained from Fisher Scientific, United Kingdom
 - a. Potassium bromide

3. Chemical obtained from BDH Chemical, England
 - a. 4-Dimethylaminobenzaldehyde
4. Chemical obtained from Prochem, United States
 - a. Acetone
5. Chemical obtained from Scharlau Chemie S.A, Europe Union
 - a. Ethanol

All chemical and reagents were used without further purification unless it is stated in the synthesis section.

3.2 Instruments

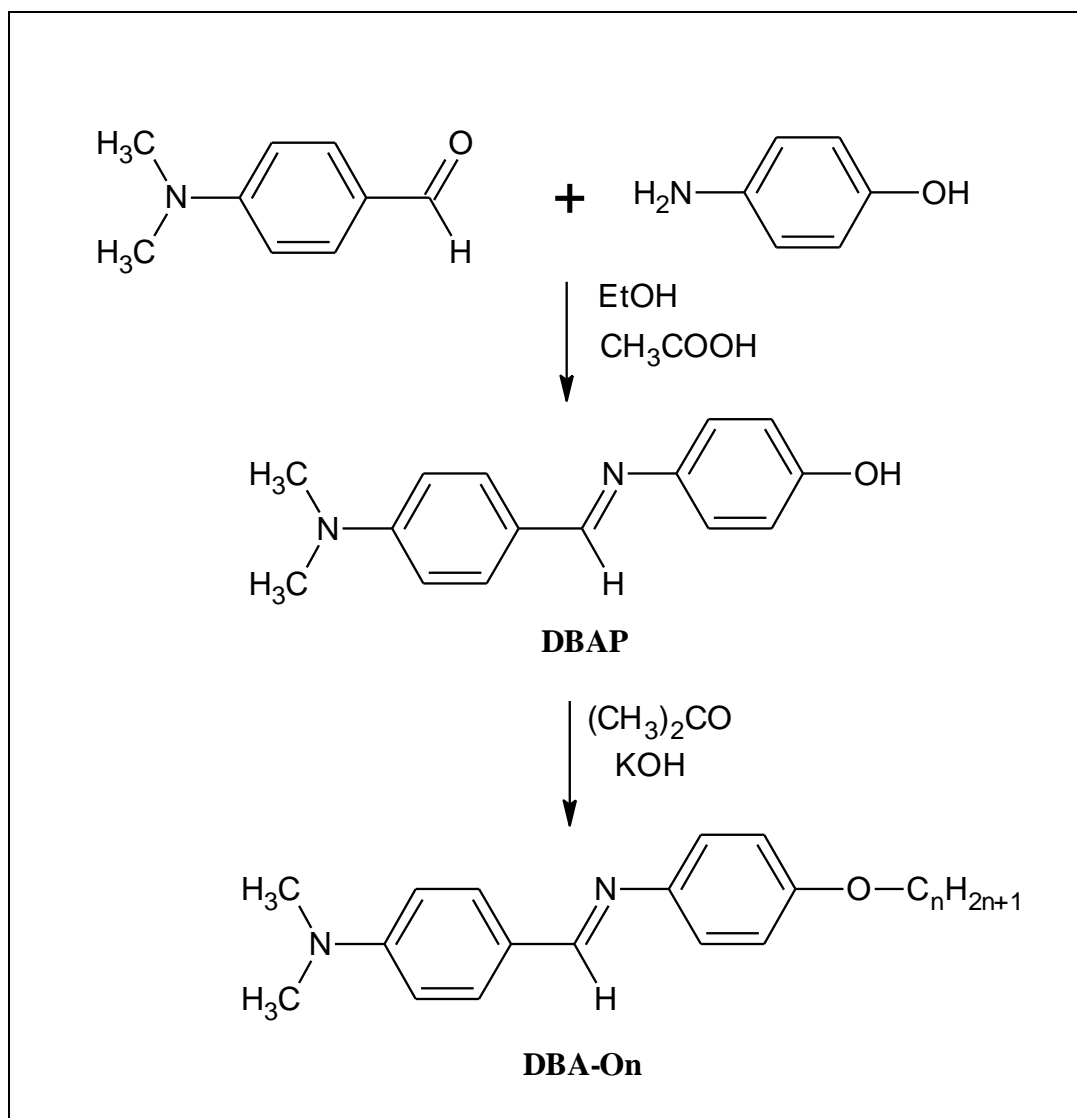
In this project, several instruments have been used to characterize properties of products. The model and the usage of the instruments are listed in the Table 3.1.

Table 3.1: Models, purpose of usages and locations of the instruments.

Model of instrument	Function	Location
Perkin Elmer 2000-FTIR Spectrometer (Spectrum RXI)	Identify useful structural information and reference to generalize characterization of functional group frequencies.	UTAR
Stuart SMP10 Melting Point Apparatus	Determine the melting point and melting range of the compounds.	UTAR
Mettler Toledo DSC823 Differential Scanning Calorimeter	To investigate the enthalpy changes and mesophase existence of the compounds.	UTAR
Bruker Avance 300 MHZ NMR spectrometer	To identify the molecular structure and dynamic of compounds.	USM
Carl Zeiss Polarizing Optical Microscope attached to Linkam Hotstage	To investigate the mesophase that found in different products.	USM
Finningam MAT95XL-T Mass Spectrometer	To identify the mass and structure of compounds by observing the fragmentation of the compound.	NUS

3.3 Synthesis

The synthesis route of **DBA-On** is shown in Figure 3.1.



where $n = 6, 8, 10, 12, 14, 16, 18$

Figure 3.1: Reaction scheme for preparing DBAP and final product, DBA-On

3.31 Synthesis of 4-[[4-(Dimethylamino)benzylidene]amino]phenol, DBAP

A solution of 4-Dimethylaminobenzaldehyde (4.48 g, 3 mmol) and 4-Aminophenol (3.27 g, 3 mmol) in 25ml of ethanol was prepared and stirred for approximately two hours under the presence of acetic acid. Yellowish solid formed was filtered and dried.

3.3.2 Synthesis of *p-n*-(Dimethylamino)benzylidene-*p*-alkyloxyanilines, DBA-On

3.3.2.1 Synthesis of *p-n*-(Dimethylamino)benzylidene-*p*-hexanoyloxyaniline, DBA-O6

4-[[4-(Dimethylamino)benzylidene]amino]phenol, (0.24 g, 1 mmol) was dissolved in acetone and subsequently subjected to Williamson etherification with 1-Bromohexane (0.17 g, 1 mmol). The solution is then heated under reflux for three hours under the presence of potassium hydroxide. The crude products formed were filtered and dried. It is then purified by repeated crystallisation from ethanol to obtain pure final product.

3.3.2.2 Synthesis of *p-n*-(Dimethylamino)benzylidene-*p*-octanoyloxyaniline, DBA- O8

The same procedures in synthesizing **DBA-O6** were repeated except that 1-Bromohexane was replaced by 1-Bromooctane (0.19 g, 1 mmol).

3.3.2.3 Synthesis of *p-n*-(Dimethylamino)benzylidene-*p* – decanoyloxyaniline, DBA- O10

The same procedures in synthesizing **DBA-O6** were repeated except that 1-Bromohexane was replaced by 1-Bromodecane (0.22 g, 1 mmol).

3.3.2.4 Synthesis of *p-n*-(Dimethylamino)benzylidene-*p*-dodecanoyloxyaniline, DBA- O12

The same procedures in synthesizing **DBA-O6** were repeated except that 1-Bromohexane was replaced by 1-Bromododecane (0.25 g, 1 mmol).

3.3.2.5 Synthesis of *p-n*-(Dimethylamino)benzylidene-*p*-tetradodecanoyloxyaniline, DBA- O14

The same procedures in synthesizing **DBA-O6** were repeated except that 1-Bromohexane was replaced by 1-Bromotetradecane (0.28 g, 1 mmol).

3.3.2.6 Synthesis of *p-n*-(Dimethylamino)benzylidene-*p*-hexadecanoyloxyaniline, DBA- O16

The same procedures in synthesizing **DBA-O6** were repeated except that 1-Bromohexane was replaced by 1-Bromohexadecane (0.31 g, 1 mmol).

3.3.2.7 Synthesis of *p-n*-(Dimethylamino)benzylidene-*p*-octadecaboyloxyaniline, DBA- O18

The same procedures in synthesizing **DBA-O6** were repeated except that 1-Bromohexane was replaced by 1-Bromooctadecane (0.33 g, 1 mmol).

3.4 Characterization

3.4.1 Infrared Spectral Analysis

Homologous series of *p-n*-(Dimethylamino)benzylidene-*p*-alkyloxyanilines, **DBA-On** was analyzed by using Perkin Elmer 2000-FTIR spectrophotometer in the frequency of 4000-400 cm^{-1} with embedded in KBr. Both identification of the functional groups frequencies and prediction of structure of the compounds can be undergone by using single beam spectrometer.

3.4.2 Differential Scanning Calorimetry (DSC)

Mettler Toledo DSC823 was used to analyze the enthalpy changes of the samples. 1-2 mg of samples were weighed and transferred to a 45 μL crucible respectively. The crucible was crimped tightly with cover by using a sealing press. The sample was then placed into the chamber of DSC instrument. The rate and temperature for both cooling and heating were set accordingly for various samples. The cooling and heating was taken under 1 ml/minutes of nitrogen flow. The sample was removed from the compartment after the scanning completed and proceeded to next sample.

3.4.3 Thin Layer Chromatography (TLC)

The sample was analyzed by using aluminum-backed silica-gel plates and examined under short-wave ultra violet light. Chloroform mixture of ethyl acetate and chloroform which acted as mobile phase was prepared with the ratio of 1:1 to dissolve the sample.

Initially, sample was dissolved in the chloroform and applied at 1cm from bottom of the TLC plate. The TLC evaporation chamber was lined with a folded piece of filter paper to create a uniform and saturated atmosphere of solvent vapor.

Besides, this can also be used to avoid evaporation of chloroform. The solvent was allowed to move until 0.5 cm from the top of TLC plate. Then, the TLC was removed and examined under short-wave ultra violet light. A pure compound will displayed only one spot on TLC plate.

3.4.4 ^1H and ^{13}C Nuclear Magnetic Resonance

NMR Bruker Avance 300 MHz UltrashieldTm was used for analyzed the ^1H and ^{13}C NMR spectroscopy of compound. CDCl_3 solvent was used to dissolve the sample at room temperature (298 K) whereas tetramethylsilane (TMS) was used as the internal standard. One of the final compounds was selected as the

representative compound to test for the ^1H NMR in the chemical shift between 0.0- 10.0 ppm and ^{13}C NMR which in the range of 0.0-200.00 ppm.

3.4.5 Mass Spectroscopy Analysis

The Electron Ionisation Mass Spectrometry (EIMS) spectrum was gained by using Finnigan MAT95XL-T Spectrometer, with ionisation electron impact in gas phase. The 70 eV electron energy is used with 200 °C of source temperature.

3.4.6 Liquid Crystal Texture and Transition Temperature Studies

Transition temperature and liquid crystal phase were observed through Carl Zeiss Polarizing Optical Microscope attached with Linkam Hostage. Firstly, the sample to be examined was transferred on the slides and covered with glass cover. The slide was then moved into the hotstage. The focus of microscope was adjusted in order to obtain an appropriate observation. The liquid crystalline texture of the products was observed under a polarizing optical microscope equipped with a hotstage and temperature regulator.

CHAPTER 4

RESULT AND DISCUSSION

4.1 Synthesis and characterization of 4-[[4 (Dimethylamino)benzylidene]amino]phenol

4.1.1 Synthesis Route of 4-[[4 (Dimethylamino)benzylidene]amino]phenol

The imination process occurs between 4-Dimethylaminobenzaldehyde and 4-Aminophenol with ethanol. The synthesis route of imination is shown in Figure 4.1 while the complete mechanism is shown in Figure 4.3.

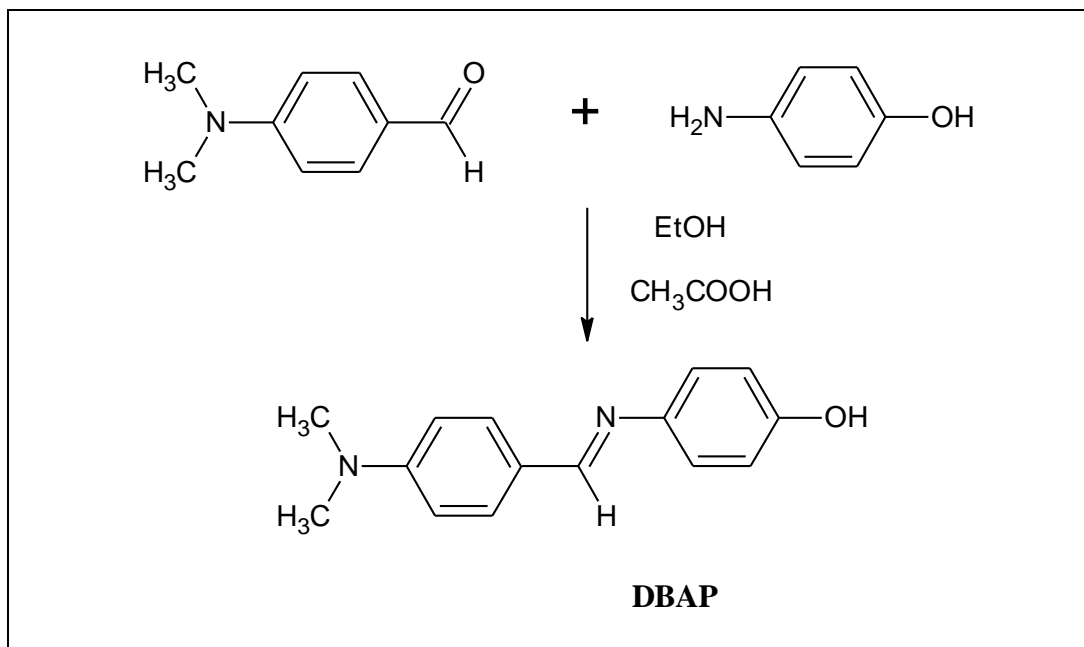


Figure 4.1: Synthesis route of Schiff base formation, DBAP

4.1.2 Fourier Transform Infra-Red Analysis of DBAP

4-[[4 (Dimethylamino)benzylidene]amino]phenol, **DBAP** is synthesized and characterized with Fourier Transform Infra-Red. The summarized IR data is tabulated in Table 4.1 and the spectra are shown in Figure 4.2.

4-Dimethylaminobenzaldehyde shows medium bands at 2903 and 2795 cm^{-1} which imply the C-H stretching bands. Methyl group has a strong bending absorption at 1370 cm^{-1} . The C=C stretching bands for aromatic ring is found to occur at 1594 cm^{-1} . There are several factors tend to influence the C=O stretching vibration, one of the factors is conjugation effect. Normally, aldehydes show a very strong bands for the carbonyl group, C=O at wavenumber 1740 – 1720 cm^{-1} . However, the conjugation of the carbonyl group with the aryl group has shifted the normal C=O stretching bands to a lower wavenumber, 1661 cm^{-1} . The C-H aldehyde stretch can be observed at 2713 cm^{-1} . The C-N stretching of aromatic amine can be found at wavenumber 1313 cm^{-1} while the aliphatic C-N stretching is found at 1163 cm^{-1} . The frequency of aromatic amines is usually higher than aliphatic amines as the resonance increases the double-bond character between the ring and attached nitrogen atom. The wavenumbers of 812 and 825 cm^{-1} indicates the substitution of C-N aromatic amines at *para* position.

4-Aminophenol exhibits a pair of N-H stretching vibration at 3341 and 3282 cm^{-1} . The asymmetric vibration and symmetric vibration cause the higher-frequency and lower-frequency respectively. In addition, the band at 3282 cm^{-1} has been enhanced by the Fermi resonance interaction with the symmetric N-H stretching band near 3341 cm^{-1} . An overtone of N-H *bending* vibration is found to

appear at 1615 cm^{-1} . At 1386 cm^{-1} , the C-N stretching for the aromatic amines can be found. The C=C stretching bands for aromatic ring is found to occur between 1559 and 1475 cm^{-1} . More useful information in the indication of phenol can be obtained through C-O stretching vibration instead of O-H bands. Phenol gives C-O absorptions at the region of 1256 cm^{-1} because of conjugation of oxygen with the ring, which shifts the band to higher energy. The present of hydrogen bonded-OH of phenol in the IR spectrum is less obvious which is at the wavenumber of 3178 cm^{-1} due to the overlapping of N-H band. The wavenumbers of 825 and 832 cm^{-1} indicate the attachment of amine at *para* position of benzene ring.

4-[[4 (Dimethylamino)benzylidene]amino]phenol, **DBAP** exhibits a weak and broad hydrogen-bonded OH at 3437 cm^{-1} . The C-O stretching vibrations of alcohol appear at the wavenumber of 1276 cm^{-1} . The sp^3 C-H stretching is found at frequency 2891 and 2778 cm^{-1} . Methyl group has a strong bending absorption at 1374 cm^{-1} . The strong absorption of $R_2C=N-R$ stretch at 1609 cm^{-1} indicates the present of imines. The strong C=C stretching bands for aromatic ring is found to occur at 1590 cm^{-1} . Besides, the C-N stretching of aromatic amines is found at 1320 cm^{-1} which has more higher wavenumber value to that of 4-aminophenol with wavenumber of 1256 cm^{-1} . This is due to the resonance effect that increases the double bond character between the benzene ring and attached nitrogen atom. The frequencies at 828 and 839 cm^{-1} indicate the attachment of functional group at *para* position of benzene ring.

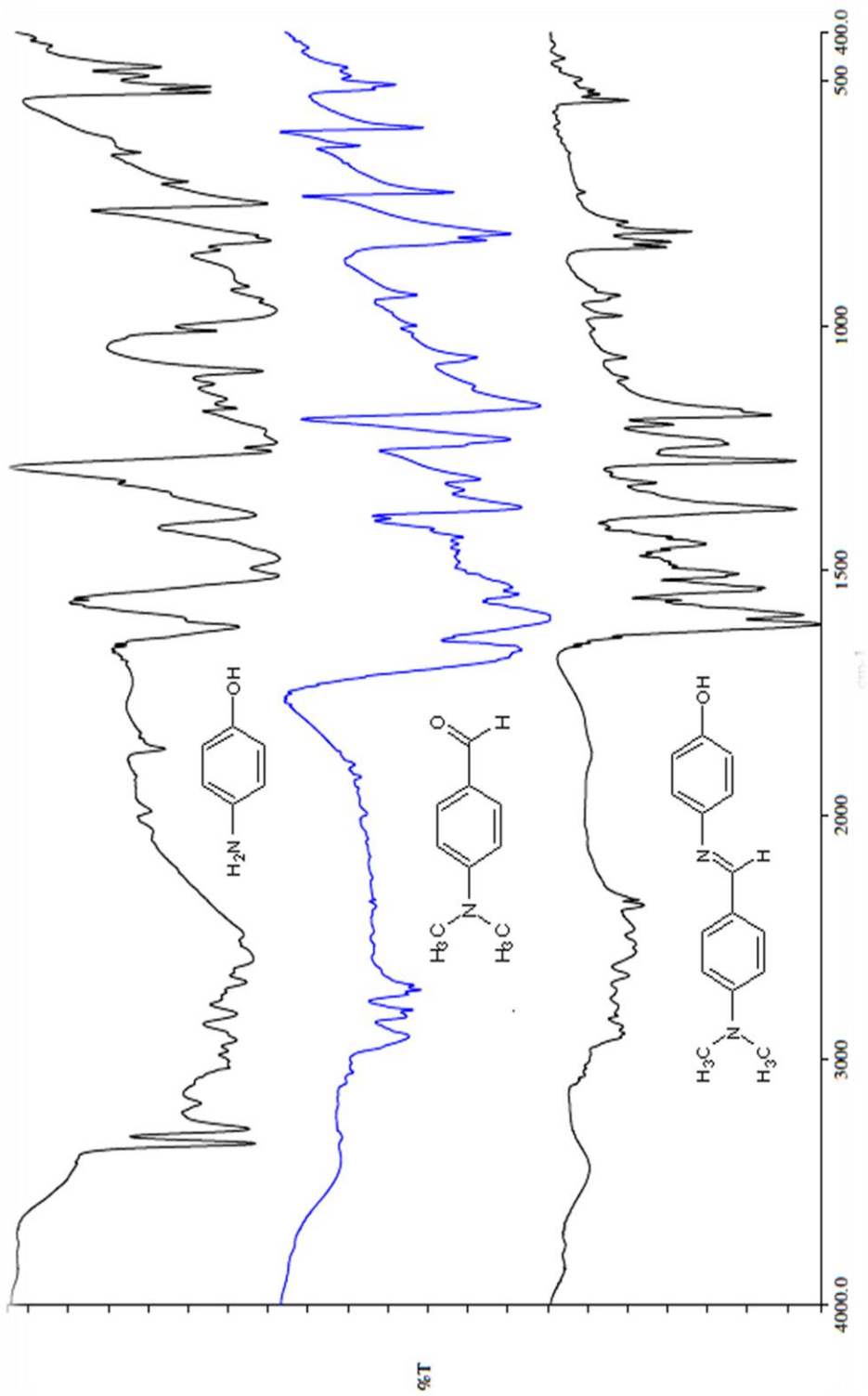


Figure 4.2: IR spectra of 4-Dimethylaminobenzaldehyde, 4-Aminophenol and DBAP

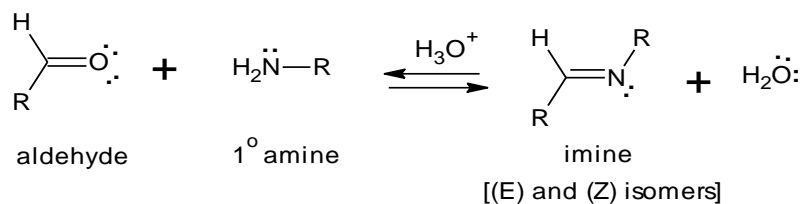
Table 4.1: IR spectra data of 4-Aminophenol, 4-Dimethylaminobenzaldehyde and DBAP

Compound	ν O-H	ν N-H	ν C-H _{ald}	ν _s CH ₃	ν C=O	δ N-H	ν C=C _{aro}	ν C=N	δ _s CH ₃	ν C-N	ν C-O	δ C-H _{oop}
4-Aminophenol	3178w	3341s 3282s	-	-	-	1615m	1510s 1475s	-	-	1386s	1256s	832m 825s
4-Dimethylamino-Benzaldehyde	-	-	2713w	-	1661m	-	1594s	-	1370s	1313m	-	825m 812s
DBAP	3437w	-	-	2891w	-	-	1590s	1609s	1374s	1320m	1276m	839w 828w

w = weak, m = medium, s = strong, ν = stretching, δ = bending, s = symmetric, oop = out-of-plane, aro = aromatic, ald = aldehyde

4.1.3 Mechanism of Imination

The process of imination process is undergone during the synthesis of **DBAP**. This process occurs between carbon atom of aldehyde, C=O and nitrogen atom of nucleophile group from 4-Aminophenol, -NH₂. Aldehydes reacts with primary amines to form compounds with a carbon nitrogen double bond called imines, either RCH=NR or R₂C=NR. The reaction is acid catalyzed and the product can form as a mixture of (E) and (Z) isomers. A new bond, imine or Schiff base is produced and water molecule as side product. The reaction can be seen as following:



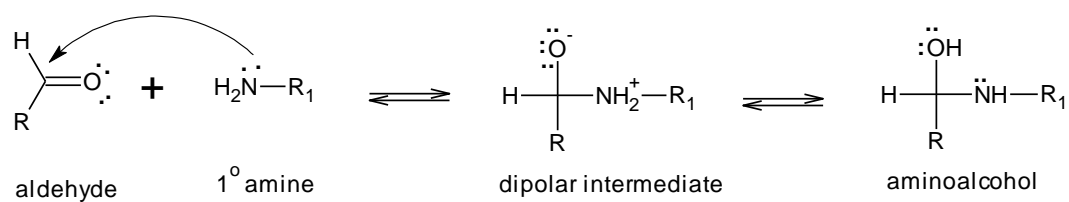
The formation of imine is slow at very low and at very high pH. The best environment for the reaction to take place is between pH 4 and pH 5 (Solomons, 2000). Hence, an appropriate amount of acetic acid which acts as acid catalyzed is added to the reaction. The mechanism of imination is shown in Figure 4.3.

In general, nucleophilic attack of amine and proton transfer forms the unstable carbolamine where H and NHR₁ are attached to the carbonyl group. The important step is the step in which the protonated aminoalcohol loses a molecule of water to become an iminium ion. By protonating the alcohol group, the acid converts a poor leaving group which an -OH group into a good one, an -OH₂⁺ group.

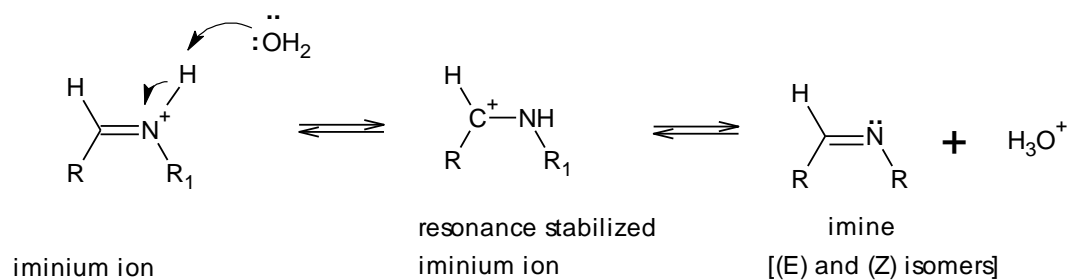
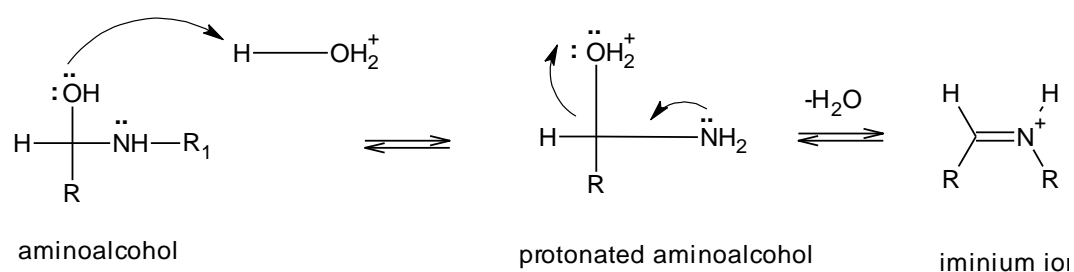
Based on Figure 4.3, in Part 1, the amine is added to the carbonyl group to form a dipolar tetrahedral intermediate. Then, an aminoalcohol is produced through the transfer of intermolecular proton from nitrogen to oxygen. In Part 2, protonation of the oxygen forms a good leaving group. Iminium ion is yielded due to loss of a molecule of water. Lastly, transfer of a proton to water forms the imine and regenerates the catalytic hydronium ion.

A too high concentration of hydronium ion will cause the reaction to proceed slowly as protonation of amine itself takes place to a considerable extent. This has the effect of decreasing the concentration of the nucleophile needed in the first step. A too low concentration of hydronium ion will cause the reaction to become slow as the concentration of the protonated aminoalcohol becomes lower (Solomons, 2000). Thus, a pH between 4 and 5 is an effective compromise.

Part 1: Nucleophilic addition forms a carbinolamine



Part 2: Elimination of water forms Imine



Where:

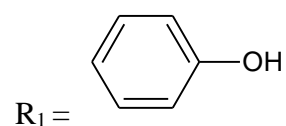
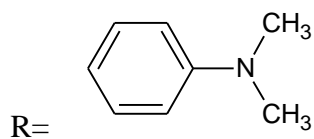
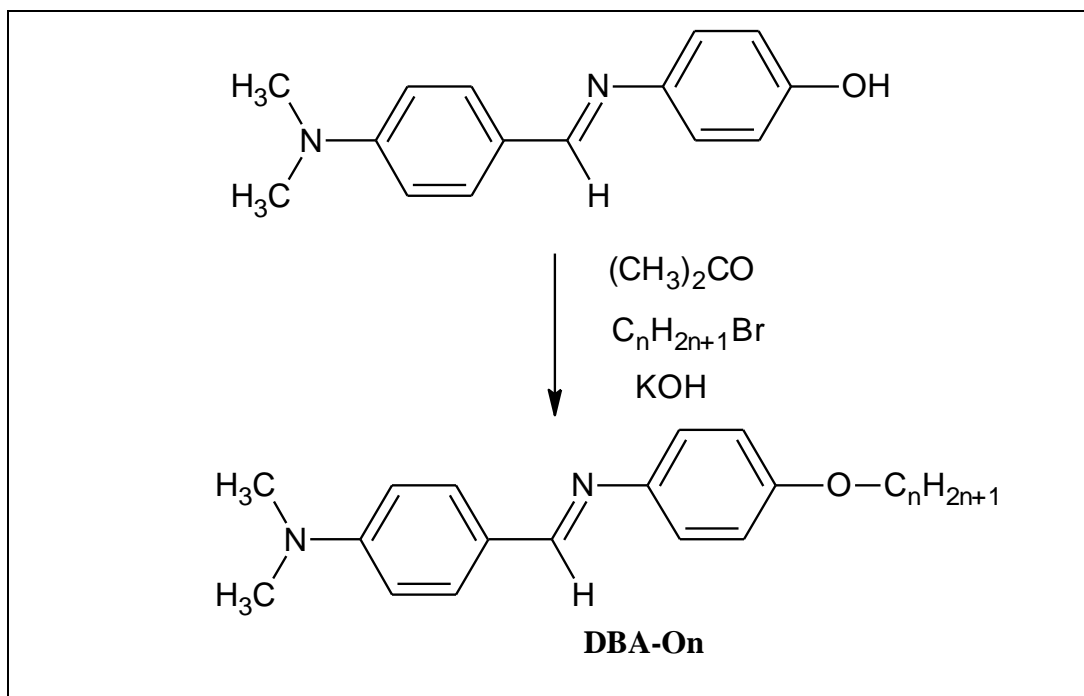


Figure 4.3: Mechanism of imination

4.2 Synthesis and Characterization of *p*-*n*-(Dimethylamino)benzylidene-*p*-alkyloxyanilines, DBA-On

4.2.1 Synthesis Route of Etherification

Etherification process occurs between the intermediate, **DBAP** and different length of bromoalkanes, $C_nH_{2n+1}Br$ to form series of **DBA-On**. Figure 4.4 shows the etherification process of **DBAP** and various lengths of bromoalkanes. **DBAP** is subjected to Williamson etherification with the bromoalkanes in the presence of potassium hydroxide. Acetone is used as solvent to dissolve **DBAP** in this process.



where $n = 2, 4, 6, 8, 10, 12, 14, 16, 18$

Figure 4.4: Etherification route between DBAP and various length of bromoalkanes

4.2.2 Infrared Spectrum Investigation on DBA-On

DBA-O16 is selected as the representative for the **DBA-On** series in the discussion. The FT-IR spectrum and data of **DBA-On** are shown in Figure 4.5 and Table 4.3.

DBA-O16 shows two sharp peaks of C-H stretch at 2918 and 2850 cm^{-1} . The presences of aromatic ring can be usually observed at 1600 cm^{-1} . However, in IR spectrum of **DBA-O16**, the ring stretch absorption at 1600 cm^{-1} is absent due to overlapping of peak with $\text{R}_2\text{C}=\text{N}-\text{R}$ stretch at 1609 cm^{-1} . The strong absorption of $\text{R}_2\text{C}=\text{N}-\text{R}$ stretch at 1609 cm^{-1} indicates the present of imines. The C-N stretching exhibits the weak absorption at 1287 cm^{-1} . Ether gives two bands in the IR spectrum which is an asymmetric C-O-C stretch at 1242 cm^{-1} and a symmetric stretch at 1024 cm^{-1} . This indicates that **DBAP** has undergone complete reaction of Williamson etherification with potassium hydroxide. The shift in the asymmetric stretching frequency in aryl ether has the higher value than in dialkyl ether as the result of resonance. The wavenumber of 835 and 813 cm^{-1} indicate the attachment of ether in the *para* position.

By comparing the IR spectrum of **DBA-O16** and **DBAP**, **DBA-O16** is found to have higher frequency of aromatic C-H stretch, which is 2919 cm^{-1} than **DBAP**, which is 2891 cm^{-1} . The increases of the electron density within the phenyl ring induced by the introduction of alkyl group into the **DBA-O16** enable the aromatic hydrogen to bind strongly to the aromatic carbon. Furthermore, it

enhances the effective charge in each aromatic C-H stretch which triggers the high frequency value of aromatic C-H stretch (Smith, 1996).

DBA-O16 is the result of etherification between **DBAP** and potassium hydroxide. The absent of O-H bond indicates the removal of water molecule which acts as side product in the etherification of process. An asymmetric C-O-C stretch at 1242 cm^{-1} and a symmetric stretch at 1024 cm^{-1} can be observed. This shows the introduction of ether group into the compound of **DBA-O16**.

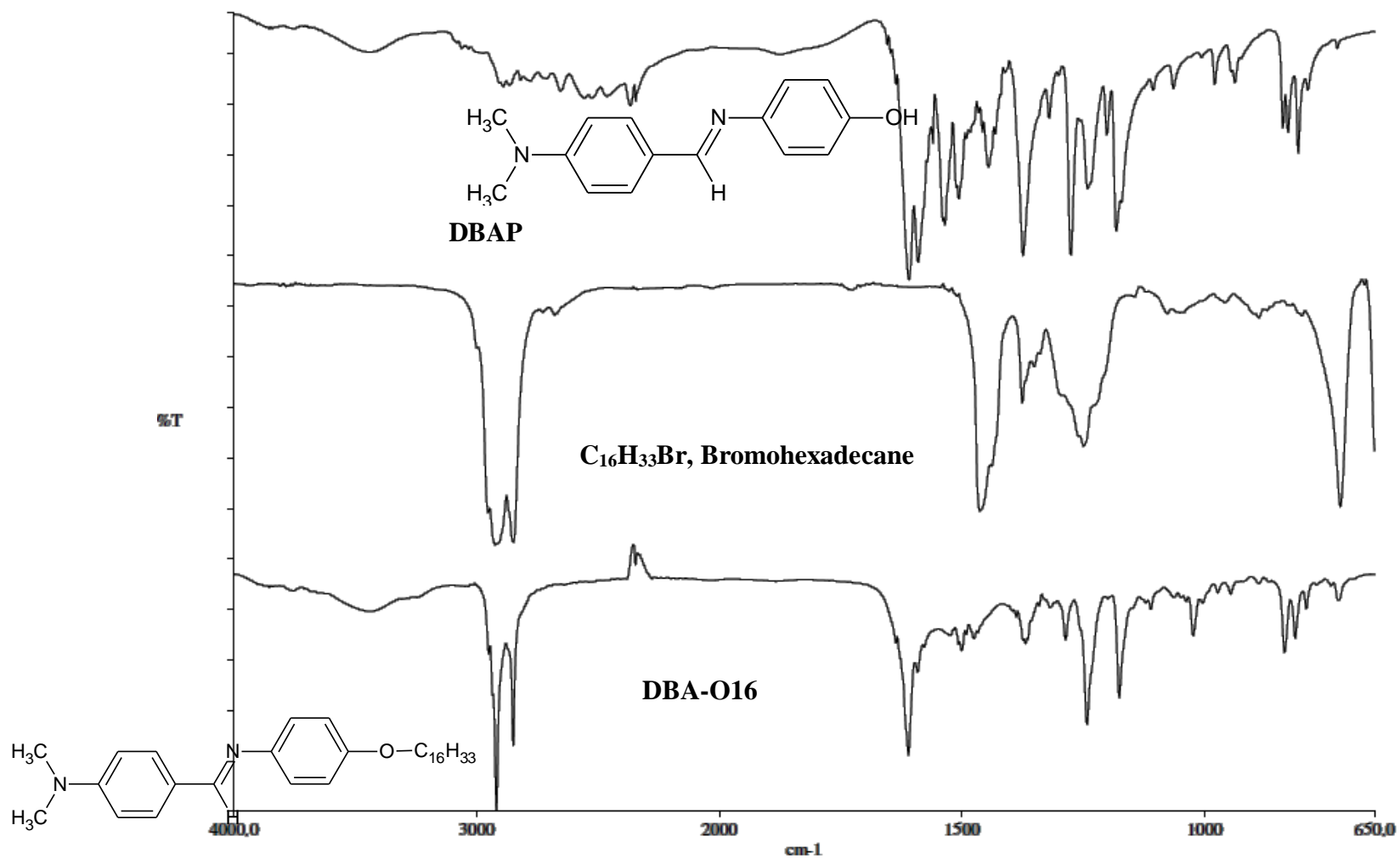


Figure 4.5: IR spectra of DBAP, Bromohexadecane and DBA-O16

Table 4.2: IR spectra data of DBAP, Bromohexadecane and DBA-O16
Table 4.2: IR spectra data of DBAP, Bromohexadecane and DBA-O16

Compound	ν O-H	ν_{as} CH ₂ ν_s CH ₂	ν_s CH ₃	ν C=N	ν C=C _{aro}	δ CH ₃	ν C-N	ν C-O	δ C-H _{oop}	C-Br
DBAP	3437w	-	2891w 2789w	1609s	1590s	1374s	1320m	1276s	839m 828m	-
Bromohexadecane	-	2924s 2853s	-	-	-	1466s	-	-	-	648m
DBA-O16	-	2918s 2850s	-	1609m	1590m	1368m	1287m	1242m	835w 813w	-

w = weak, m = medium, s = strong, ν = stretching, δ = bending, s = symmetric, as = asymmetric, oop = out-of-plane, aro = aromatic

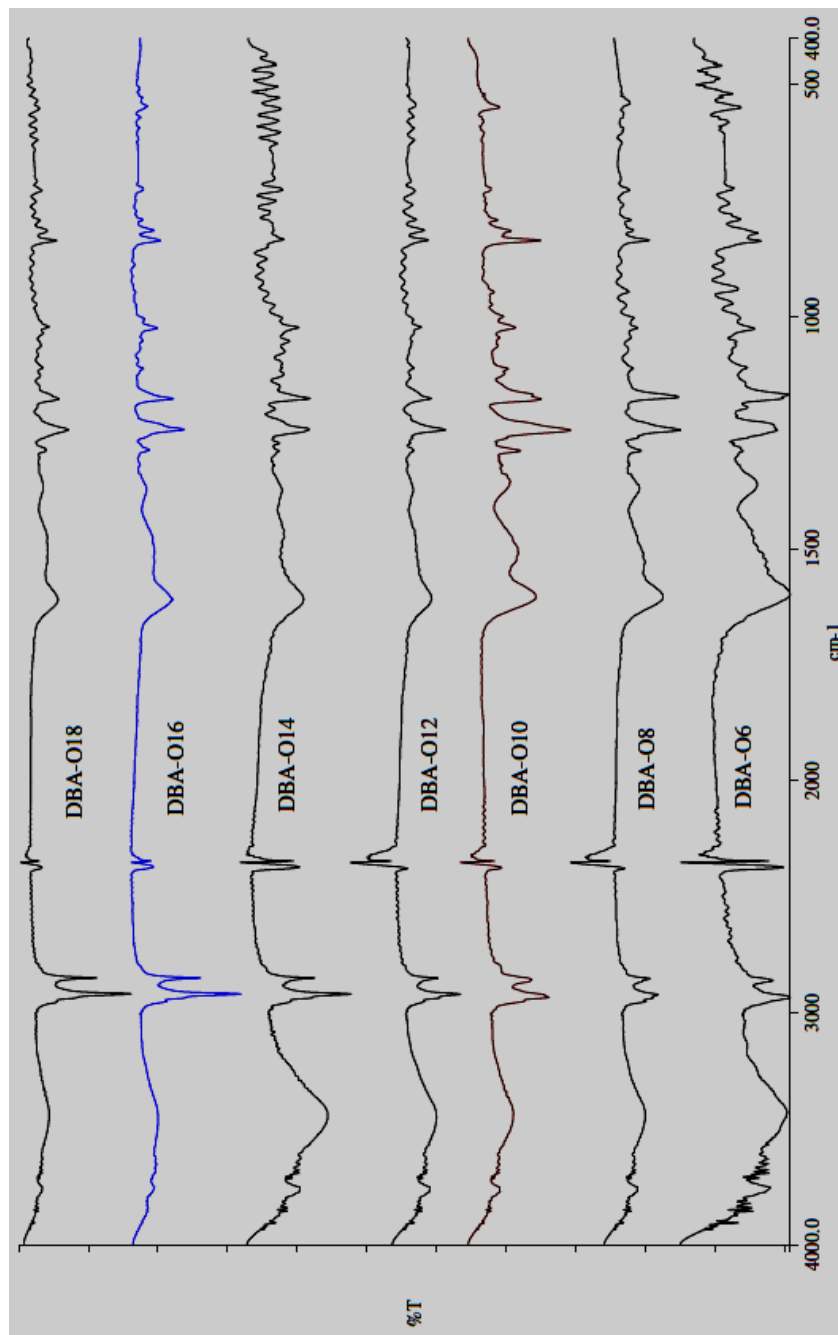


Figure 4.6: IR Spectra of DBA-On, n= 6, 8, 10, 12, 14, 16 and 18

Table 4.3: IR spectra data of DBA-On where n = 6, 8, 10, 12, 14, 16 and 18

Compound	$\nu_{\text{as}}\text{CH}_2$ $\nu_{\text{s}}\text{CH}_2$	$\nu\text{C}=\text{N}$	δCH_3	$\nu\text{C}-\text{N}$	$\nu\text{C}-\text{O}$	$\delta\text{C}-\text{H}_{\text{oop}}$
DBA-O6	2934m 2856m	1603m	1363m	1288w	1240s	836w 816m
DBA-O8	2921m 2853m	1602m	1363m	1288w	1243s	835w 812m
DBA-O10	2933m 2856m	1604m	1367m	1288m	1244s	835w 812w
DBA-O12	2919s 2850m	1608m	1368m	1284m	1243m	834w 814w
DBA-O14	2918s 2850m	1608m	1368m	1270m	1242m	813w 809w
DBA-O16	2919s 2850s	1609m	1368m	1287m	1242m	835w 813w
DBA-O18	2919s 2850s	1608m	1368m	1284m	1243m	814w 812w

w = weak, m = medium, s = strong, ν = stretching, δ = bending, s = symmetric, as = asymmetric, oop = out-of-plane, aro = aromatic

4.2.3 Mechanism of Williamson Etherification

Williamson etherification is a S_N2 reaction between an alkoxide, RO^- ion and an alkyl halide, $R'X$ giving an ether. When the two ether is identical, the ether is a symmetric ether, and when two R group are different, the ether is an asymmetric ether.

In planning the Williamson ether synthesis, it is essential to use a combination of reactants that maximizes nucleophilic substitution and minimizes any competing β -elimination (Brown *et al.*, 2009). Yields of ether are highest when the halide to be displaced to a methyl or a primary carbon. Yields are low in a displacement from secondary halides because of the competing of β -elimination. The Williamson etherification fails to be carried out with tertiary halides as β -elimination by an E2 mechanism is an exclusive reaction (Brown *et al.*, 2009).

In the first step of the reaction, an alcohol is deprotonated usually by the addition of strong base. Sometimes, sodium metal is used as well in the deprotonation of alcohol. In the second step, a primary alkyl halide is added and gets an S_N2 reaction in which the alkoxide undergoes the nucleophilic attack to displace the halide.

The Schiff base intermediate, **DBAP** is subjected to Williamson etherification with the suitable bromoalkanes in the presence of potassium hydroxide. The proposal mechanism for the Williamson etherification is shown in Figure 4.7.

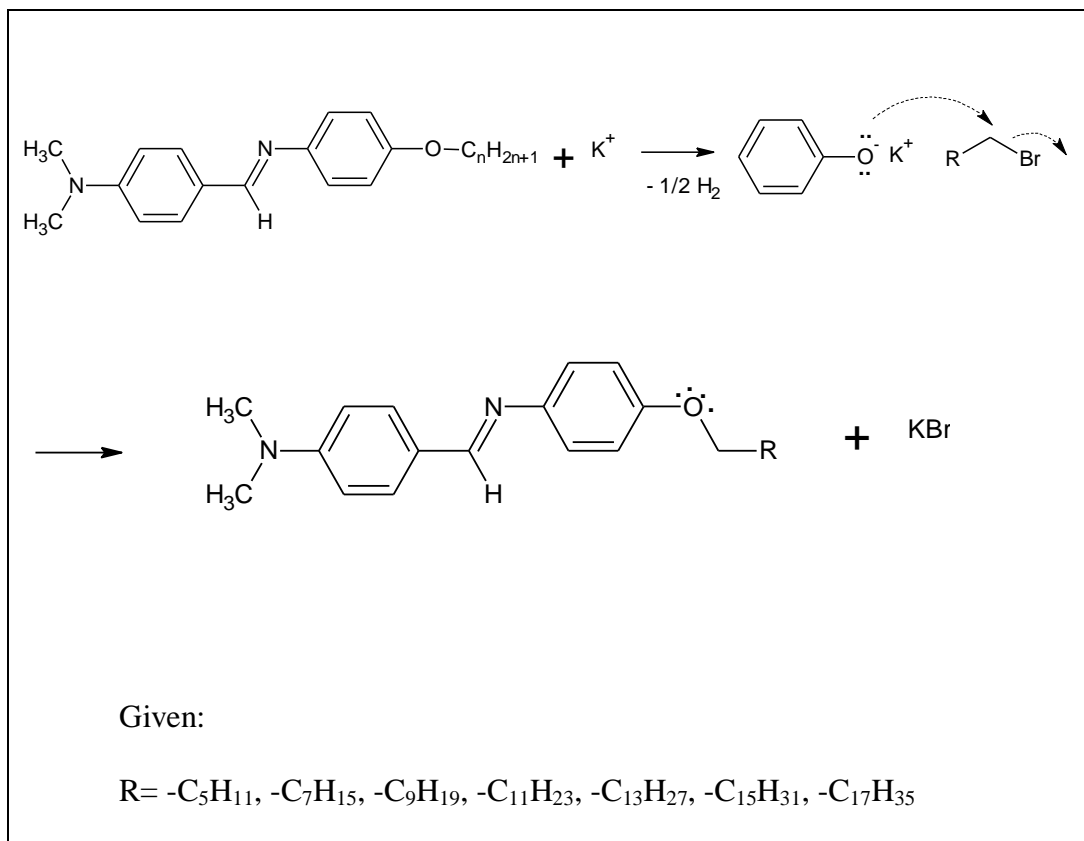


Figure 4.7: Mechanism of the Williamson Etherification

4.2.4 Nuclear Magnetic Resonance Analysis

4.2.4.1 ^1H NMR Spectrum Analysis

The structure and purity of the synthesized compound are confirmed by using ^1NMR analysis techniques. The structure and ^1NMR spectrum of **DBA-O16**, with its numbering are shown in Figure 4.8. The data is tabulated in Table 4.4. The result analysis for compound **DBA-O16** is discussed as the representative of the series of **DBA-On**.

The most upfield signal observed at $\delta = 0.9$ ppm due to the methyl protons attached to the sp^3 carbon, H1 which is chemically and magnetically equivalent. It also shows no electronegative element or π -bonded group are close to the hydrogen. Another multiplet signal can be studied in the range of $\delta = 1.27$ - 1.48 ppm which owing to the methylene groups, H2-H14. All of the CH and CH₂ in long hydrocarbon chains may overlap in an irresolvable group. The chemical shift values of hydrogens in methyl group are lower than methylene or methine hydrogens due to its highly shielded type of proton. H15 exhibits chemical shift value of 1.8 ppm with quintet signals which caused by the phenomenon of spin-spin splitting. Due to (n+1) rules, four adjacent protons in between H15 affecting the splitting of H15.

The chemical shift of the $-\text{N}(\text{CH}_3)_2$ hydrogen, H22 is shown at 3.06 ppm with a singlet signal. Besides, the peak of H16 is found at $\delta = 4.00$ ppm which

indicates the presence of the hydrogen of ether. In ether, the hydrogens on the carbon next to oxygen are deshielded due to the electronegativity of the attached oxygen. Azomethine proton, H19 has the most deshielded signal which appears as a singlet with the chemical shift value of 8.36 ppm. The appearance of a singlet signal is due to the absence of adjacent protons. Moreover, H19 is shifted to a downfield probably caused by the electron withdrawing effect of the nitrogen atom.

Generally, the hydrogens attached to aromatic rings can be easily observed in the chemical shift region from 6.50 to 8.00 ppm. The great chemical shift of the benzene ring is due to the anisotropy effect. The aromatic protons, H17 show a doublet signal at $\delta = 7.78$ ppm while the doublet signals of H18 are shown at $\delta = 7.20$ ppm. Both aromatic protons have the coupling constant of 8.8 Hz which indicates the presence of a proton at the *ortho* position of H17 and H18 respectively. H17 has the chemical shift value higher than H18. This is due to the electron withdrawing effect of the nitrogen atom.

For H20 and H21, the doublet signals occur at $\delta = 6.90$ ppm and $\delta = 6.73$ ppm respectively. As compared to both aromatic protons, the chemical shift value of H21 is lower than H20 due to the shielding effect from the electron donating effect of $-\text{N}(\text{CH}_3)_2$ to the ring. The coupling constant of both H20 and H21 is 8.8 Hz, therefore, the proton is attached to the *ortho* position of H20 and H21 correspondingly.

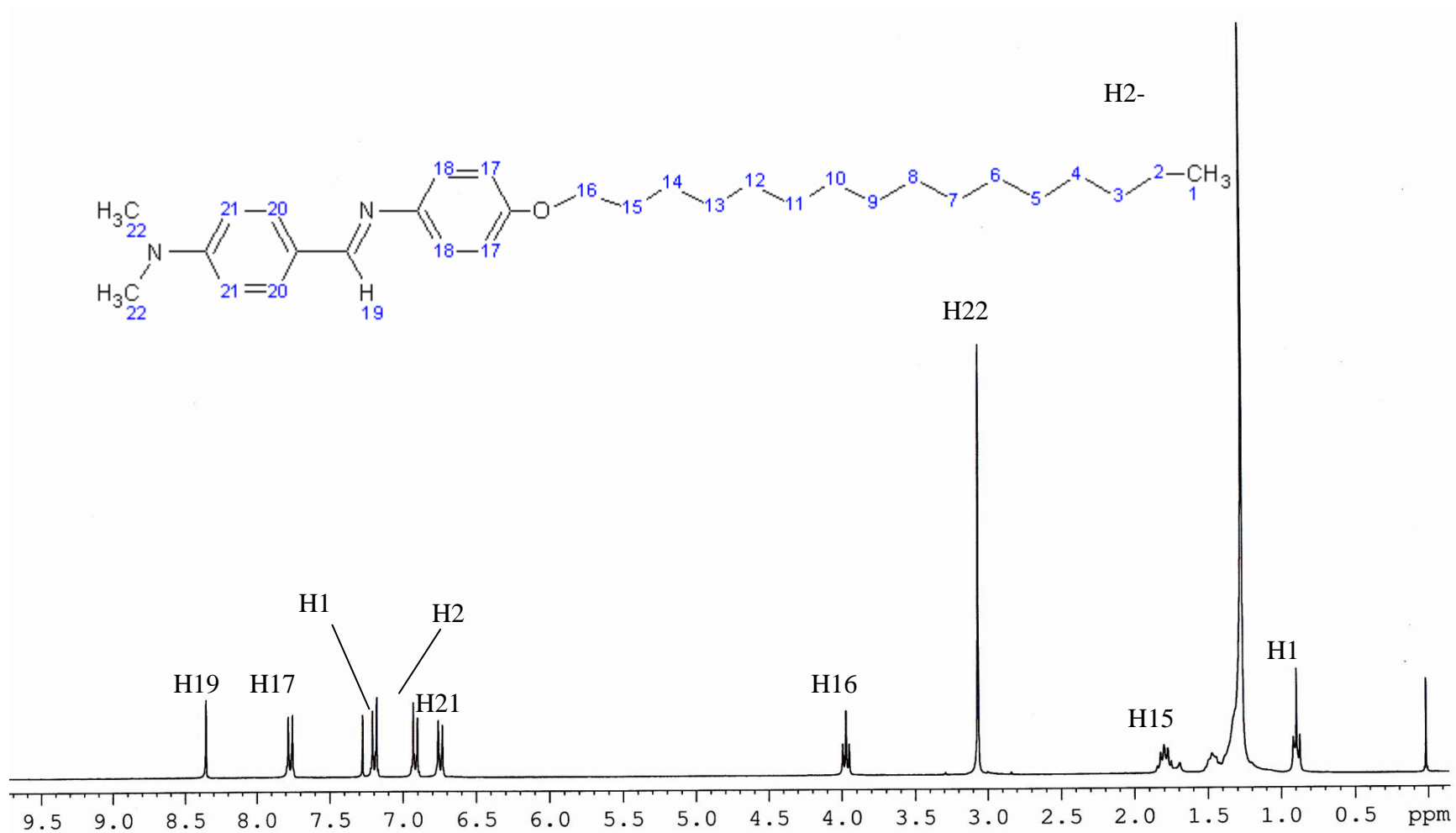
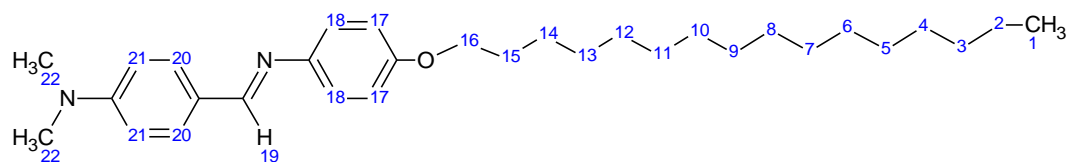


Figure 4.8: ¹H NMR spectrum of *p-n*-(Dimethylamino)benzylidene-*p*-hexadecanoyloxylaniline, DBA-O16

Table 4.4: ^1H NMR spectrum of *p*-*n*-(Dimethylamino)benzylidene-*p*-hexadecanoyloxylaniline, DBA-O16



Protons	Number(s) of H	Coupling Constant, J(Hz)	Chemical Shift, ppm	Peak (s)
H1	3	-	0.90	t
H2-H14	30	-	1.27-1.48	m
H15	2	-	1.80	q
H22	6	-	3.06	s
H16	2	-	4.00	t
H21	2	8.8	6.73	d
H20	2	8.8	6.90	d
H17	2	8.8	7.78	d
H18	2	8.8	7.20	d
H19	1	-	8.36	s

TMS as internal standard; CDCl_3 as solvent; s, singlet; d, doublet; t, triplet, q, quintet; m, multiplet

4.2.4.2 ¹³C NMR Spectrum Analysis

The structure and purity of the synthesized compound are confirmed by using ¹³C NMR analysis techniques. The structure and ¹³C NMR spectrum of **DBA-O16**, with its numbering is shown in Figure 4.9. The data is tabulated in Table 4.5. The result analysis for compound **DBA-O16** is discussed as the representative for this series of compound.

The signal appears at the most downfield region at $\delta = 159.1$ ppm is attributed to CH=N azomethine carbon, C21. The azomethine carbon appears in a range farther downfield is due to the strong electronegativity of nitrogen atom which pulls the electron toward itself from the carbon. A signal observed at $\delta = 158.4$ ppm is assigned to C17, the ipso carbon next to the oxygen atom whereas C20, α carbon towards the azomethine linkage is seen at $\delta = 151.0$ ppm. C20 has the chemical shift value lower than C17 as it is attached to the strong electronegativity of oxygen atom. The signal at $\delta = 122.5$ ppm shows the attachment of C19 at *ortho* position in benzylidene ring towards the azomethine linkage. The signal at $\delta = 130.9$ ppm is ascribed to equivalent carbon C18 which is in the *meta* position towards the azomethine linkage. C19 has the similar reason as C20, hence, it has lower chemical shift value than C18. Both C18 and C19 have the higher intensities than C20 and C17 due to the NOE effect of the heteronuclear interaction between the C-H atoms.

The signal at $\delta = 148.5$ ppm and $\delta = 124.5$ ppm are attributed to C22 and C25 respectively. C22 shows higher chemical shift than C25 owing the existence of double bond and higher electronegativity of nitrogen atom. In addition, the electronegativity of nitrogen atom which attached to C25 is weakening by the electron donating group attached to it. Hence, the chemical shift value of C25 is lower. The peaks at $\delta = 122.2$ ppm and $\delta = 112.0$ ppm indicate C23 and C24 respectively. As the NOE effect is applicable in the aromatic carbon-hydrogen interaction, therefore, it gives higher intensities of signal than C22 and C25. At $\delta = 32.9$ ppm, C26, the methyl group next to the nitrogen atom is observed. C26 has the higher chemical shift than aliphatic carbon as it is attached to the nitrogen atom which is an electron withdrawing group.

The chemical shift $\delta = 14.1 - 40.1$ ppm, C1-C15 is ascribed to the alkyl long chain. C15 has the most downfield in this range as it is attached to the carbon of ether located next to it. The $\delta = 14.1, 22.6, 26.0$ and $29.3 - 31.9$ ppm respectively is indicated as alkyl long chain after C15. Intensities of these alkyl long chains are high due to signal enhancement effect and the interaction of the spin-spin dipoles operated via space. The signal emerges at the middle of the region, C16 with $\delta = 68.2$ ppm is assigned to carbonyl group, ether C-O-C.

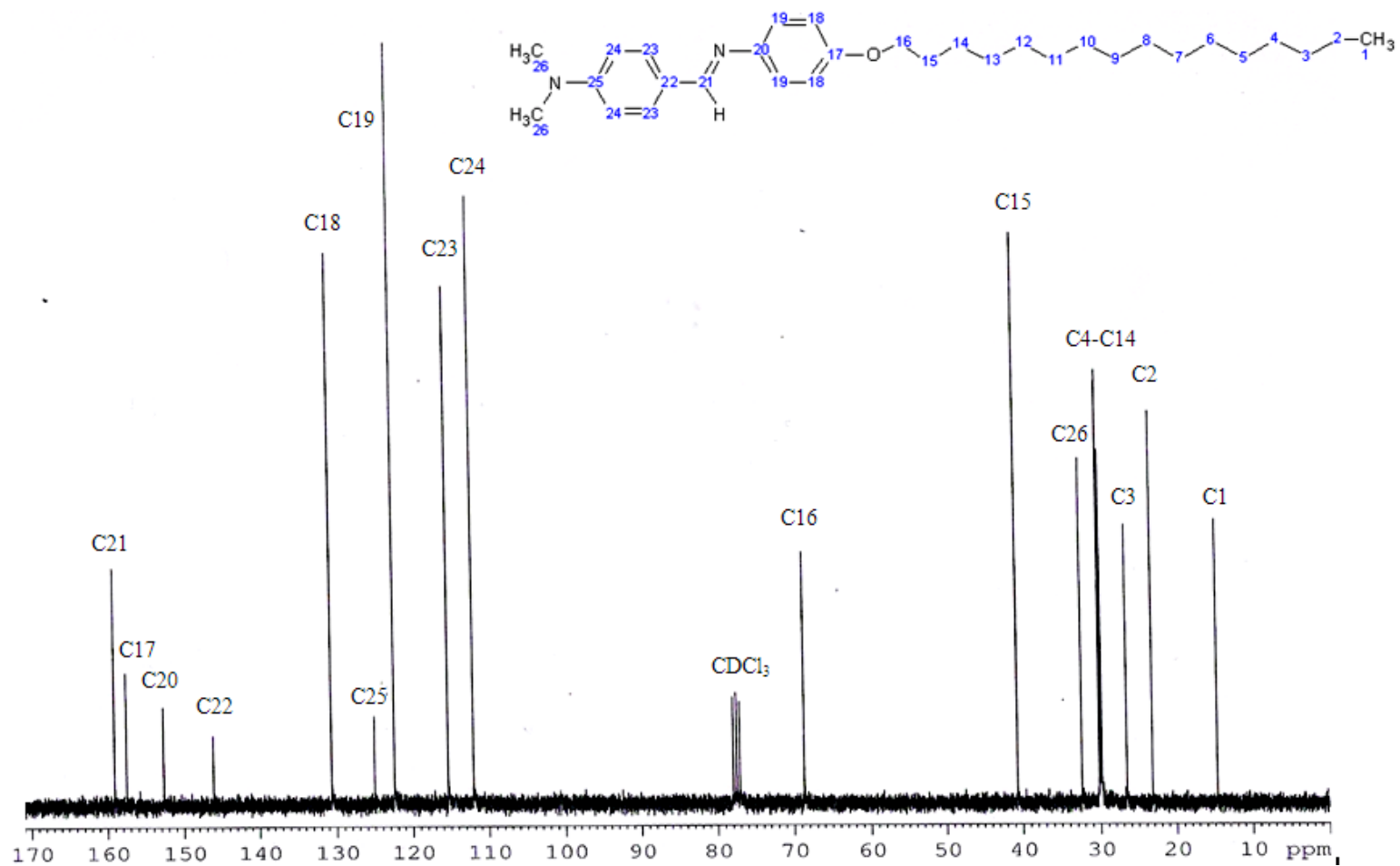
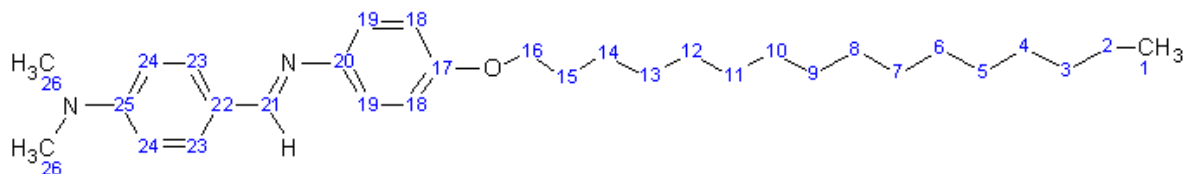


Figure 4.9: ^{13}C NMR spectrum of *p-n*-(Dimethylamino)benzylidene-*p*-hexadecanoyloxylaniline, DBA-O16

Table 4.5: ^{13}C NMR spectrum of *p*-*n*-(Dimethylamino)benzylidene-*p*-hexadecanoyloxyaniline, DBA-O16



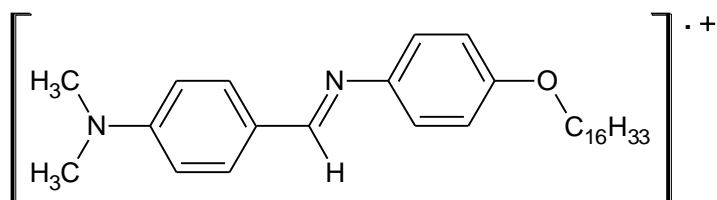
Position of Carbon (s)	Chemical shift (ppm)
C1	14.1
C2	22.6
C3	26.0
C4-C14	29.3-31.9
C26	32.9
C15	40.1
C16	68.2
C24	110.3
C23	110.6
C19	121.9
C25	124.7
C18	130.1
C22	145.7
C20	152.2
C17	158.4
C21	159.1

TMS used as internal standard; CDCl_3 as solvent

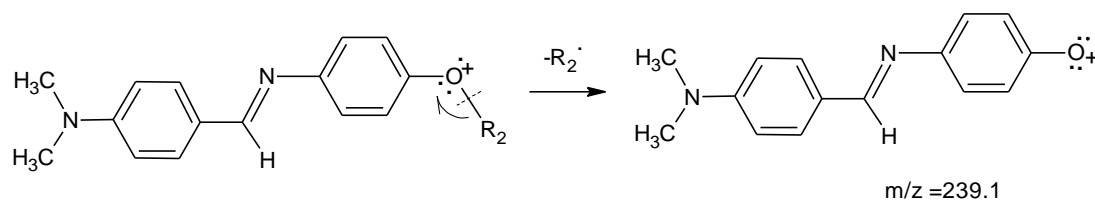
4.2.5 Mass Spectroscopic Analysis

The structure and purity of the synthesized compound are confirmed by using EI-Mass Spectroscopic analysis techniques. The structure of respective compound, **DBA-O16** is selected as representative of the series of **DBA-On** in the discussion. The m/z value and the proposed fragments of the compound are tabulated in Table 4.6.

Molecular ion peak, M^+ for **DBA-O16** is discernible. It appears at $m/z=464.4$

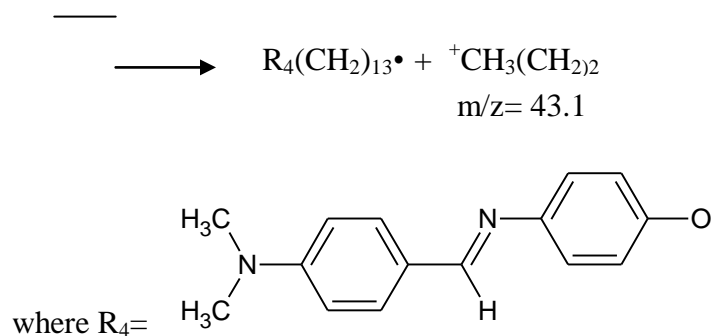


The most abundant ion formed in the ionization chamber gives rise to highest peak in the mass spectrum known as the base peak. In the mass spectrum of **DBA-O16**, the base peak is arisen at $m/z=239.1$ due to the elimination of alkyl chain of phenyl ether. The fragmentation pattern is shown as below:



where $\text{R}_2 = \text{OC}_{16}\text{H}_{33}$

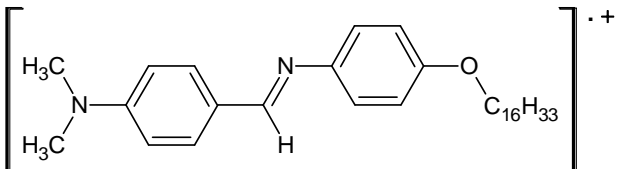
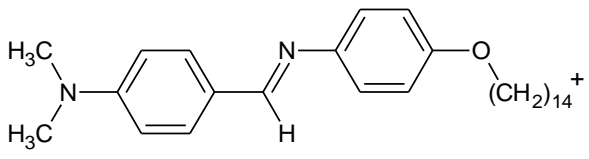
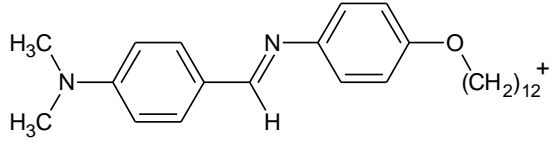
Another signal arises at $m/z = 195.0$ indicate the elimination of alkyl chain of phenyl ether and dimethylamino.



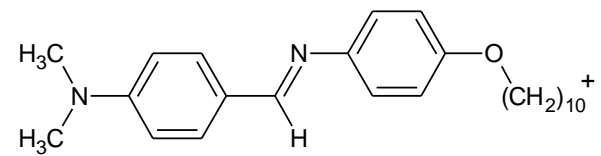
The fragments of alkyl chain of ether are fragmented by one bond σ cleavage.

This cleavage at C-C produces cation and radical (Hoffmann and Stroobant, 2005).

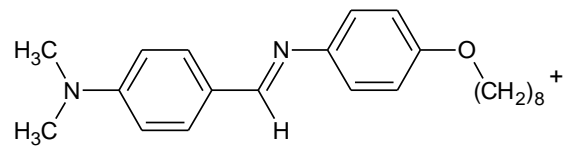
Table 4.6: m/z value and the proposed fragment of DBA-O16

m/z	Proposed Fragment
464.4	
435.3	
407.3	

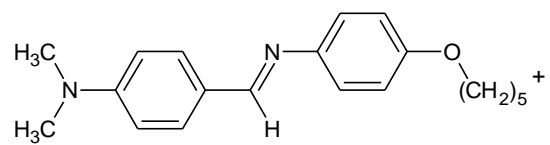
379.2



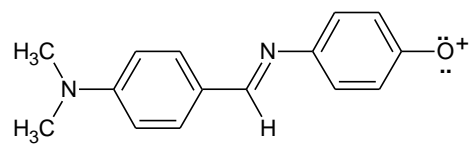
351



309



239.1



71



43



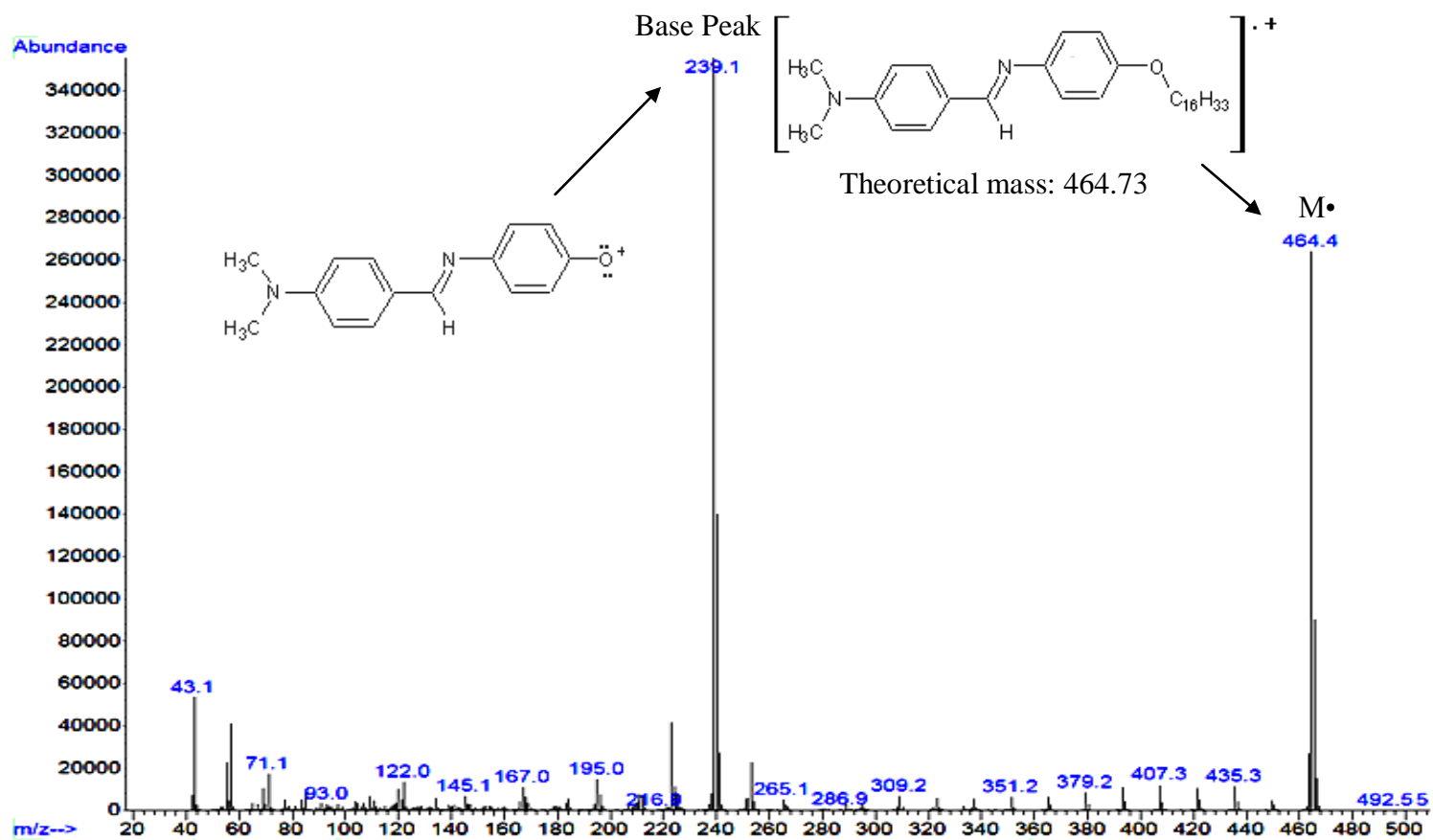


Figure 4.10: EI-Mass spectrum of *p-n*-(Dimethylamino)benzylidene-*p*-hexadecanoyloxyanilines, DBA-O16

4.3 Mesomorphic Behaviour Analysis

4.3.1 Polarizing Optical Microscope Analysis

The mesomorphic behaviour of **DBA-On** series, the benzylideneanilines are studied under the polarizing optical microscopy. Both **DBA-O6** and **DBA-O12** are selected as the representative compound. The mesophase properties are shown under the cooling process instead of heating process. **DBA-O6** to **DBA-O12** exhibits monotropic behavior whereas **DBA-O14** to **DBA-O18** is non-mesogens. All the mesogens consist of homeotropic and homogeneous alignment. The result and optical photomicrograph are shown in Figure 4.11a, 4.11b and 4.12.

Two basic forms of alignment for liquid crystalline compounds can be observed when evaluating the physical properties of liquid crystals under the microscope, homeotropic and homogeneous (planar). Homeotropic texture refers to mesogen configuration in which the alignment of molecules are normal to the supporting substrate. When the molecules are so orientated, polarized light is unaffected by the material and light cannot pass through. Thus, an area of complete blackness can be seen under POM observation.

In homogeneous (planar) alignment, the molecules are oriented parallel to the supporting substrates. A thin film of liquid crystals exhibits birefringence and a coloured texture results can be observed under POM (Collings and Hird, 1997). In fact, the alignment of molecules is influenced by the thickness of sample. Thin

samples tend to form homeotropic alignment whereas thicker samples tend to some regions of homeotropic alignment and some regions of homogeneous alignment (Collings and Hird, 1997). Mesophase identification of a compound can be simplified by having two textures to confirm identity rather than just one that may be exhibited.

Under polarizing microscope, **DBA-O12** exhibits monotropic nematic phase. The mesophase is identified by the nematic droplets texture. The mesophase sequence is from isotropic \longrightarrow nematic phase as shown in Figure 4.11a. When cooling down from the isotropic liquid, birefringent droplets occur against a black background as the nematic phase is formed. Homeotropic texture can be found under polarizing microscope due to the use of thin sample of a material as shown in Figure 4.11b. On top of that, an intense Brownian motion, a characteristic of nematic phase is observed due to the high degree of disorder of the phase structure.

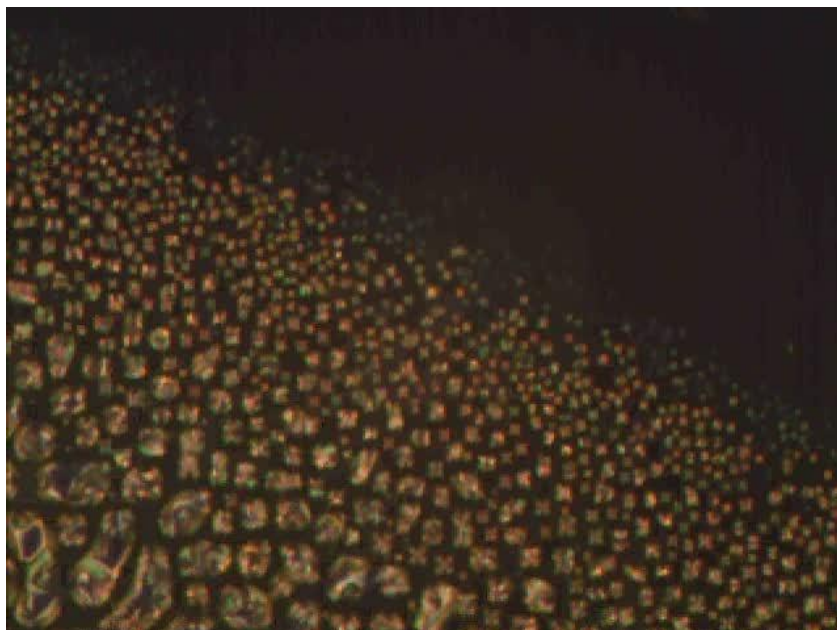


Figure 4.11a): Optical photomicrograph of DBA-O12 undergoes phase transition of isotropic to nematic during its cooling cycle

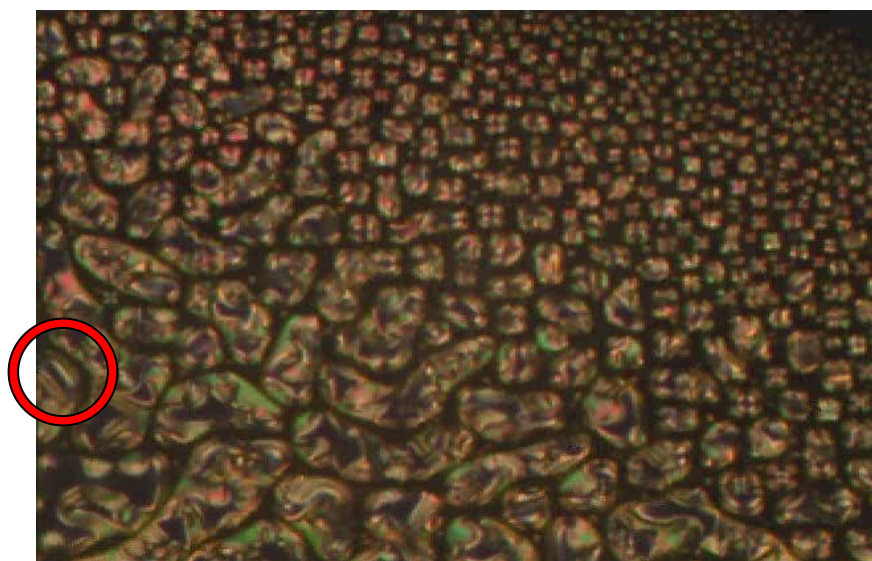


Figure 4.11b): Optical photomicrograph of DBA-O12 exhibiting nematic droplets texture and homeotropic texture (in red circle) during its cooling cycle

DBA-O6 shows a monotropic nematic phase as well under POM. The mesophase is identified by the nematic droplets texture. The mesophase sequence



is from isotropic nematic phase. The homeotropic texture which is optically extinct and an intense Brownian motion can be observed under POM.

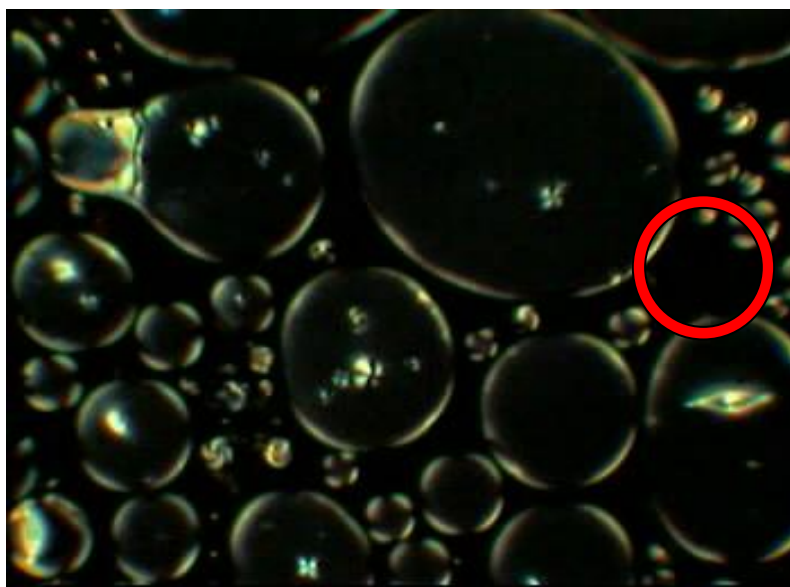


Figure 4.12: Optical photomicrograph of DBA-O6 exhibiting nematic droplets texture and homeotropic texture(in red circle) during its cooling cycle

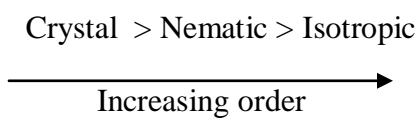
4.3.2 Differential Scanning Calorimetry Thermogram Analysis

The transition temperature and enthalpy changes are investigated by using Differential Scanning Calorimetry analysis technique. The representative DSC thermogram of **DBA-O12** is shown in Figure 4.13. The data is tabulated in Table 4.7.

A sharp peak is observed at 96.86 °C (55.85 kJmol⁻¹) for heating cycle. **DBA-O12** exhibits an endotherm corresponding to the direct melting of the crystal phase to the isotropic liquid phase during the heating cycle. The adsorbed endothermic energy is used to break apart the intermolecular force between molecules. As for cooling cycle, there are two peaks can be observed. The relative small peak at 89.59 °C (1.14 kJmol⁻¹) indicates the changes of isotropic → nematic phase. The sharp peak at 83.06 °C (45.33 kJmol⁻¹) represents the phase transition from nematic phase to crystal phase. As crystallization of the compound is known to be exothermic process, hence, energy is released during the formation of its intermolecular forces.

The magnitude of enthalpy changes is proportional to the change in structural ordering of phases involved (Collings and Hird, 1997). By studying the cooling cycle, the changes of enthalpy from the phase transition of the isotropic liquid phase to nematic phase is 1.14 kJmol⁻¹. A relatively low energy is needed to change the disoriented molecules in isotropic liquid phase to more oriented molecules of nematic phase.

The conversion of nematic phase to crystal gives 45.33 kJmol^{-1} . A sufficient amount of energy is needed to be released to gain a complete crystalline arrangement with strong intermolecular force. Hence, the enthalpy energy is relatively high. The mesophase of **DBA-O12** only occurs during the cooling cycle. Thus, it can be concluded that **DBA-O12** is a monotropic nematogen. The tendency of the series to supercool before they recrystallise enables the nematic phase to be exhibited as a metastable state below the melting point (Collings and Hird, 1997). As data provided, the molecular orientation is as following:



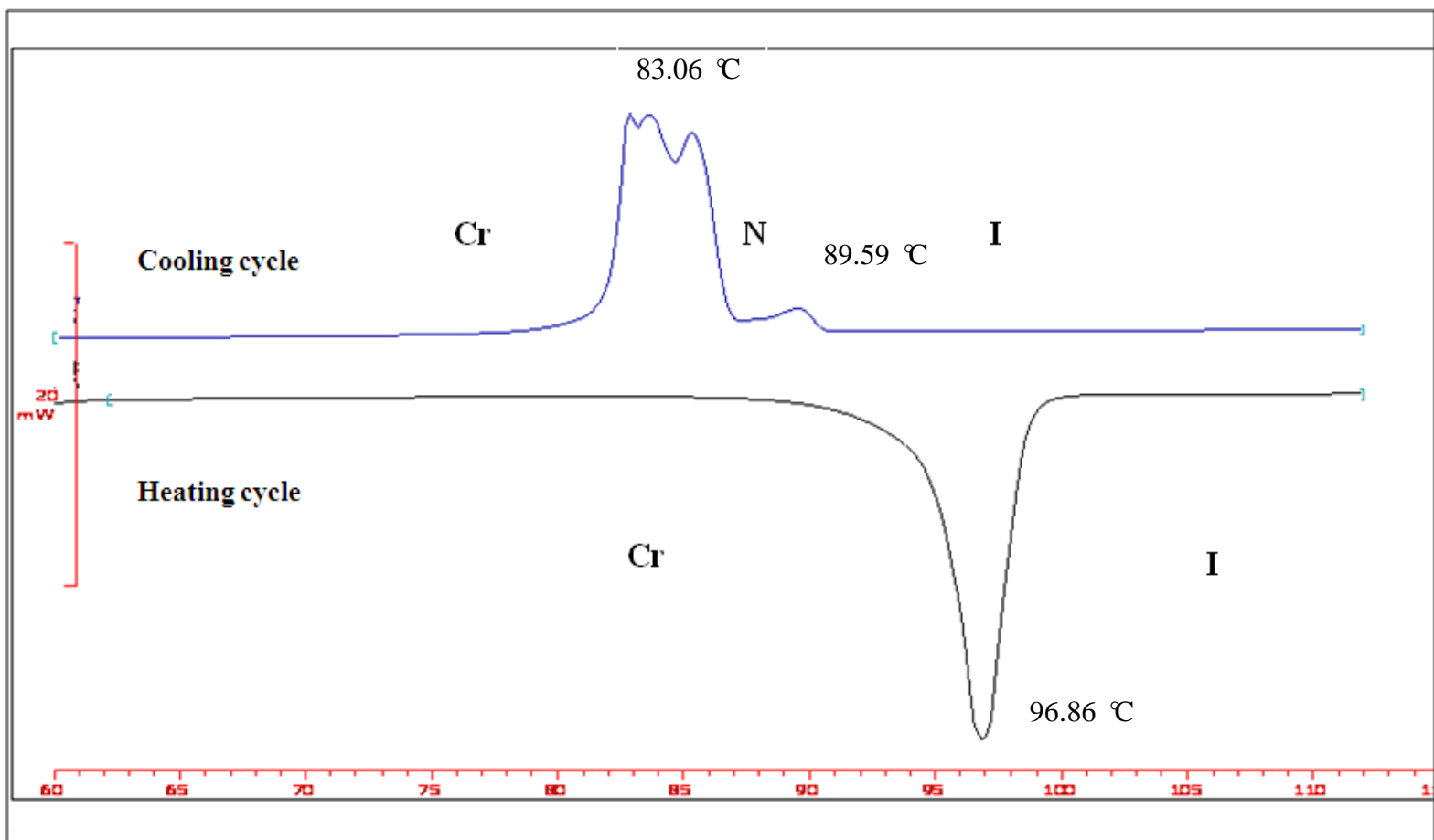


Figure 4.13: DSC Thermogram for DBA-O12

Table 4.7: Transition temperatures of compounds DBA-On, where n = 6, 8, 10, 12, 14, 16 and 18, upon heating and cooling, obtained from DSC

Compound	Transition	Temperature (°C)	Phase Range (°C)	$ \Delta H $ (kJ mol ⁻¹)
DBA-O6	Cr→I	110.13	-	37.58
	I→N	85.93	2.80	0.42
	N→Cr	83.13		33.40
DBA-O8	Cr ₁ →Cr ₂	80.37	-	22.06
	Cr ₂ →I	93.00	8.66	1.10
	I→N	91.23		23.74
	N→Cr	82.57		
DBA-O10	Cr→I	83.63	-	29.68
	I→N	75.87	3.30	0.04
	N→Cr	72.57		11.34
DBA-O12	Cr→I	96.86	-	55.85
	I→N	89.59	2.90	1.14
	N→Cr	83.06		45.33
DBA-O14	Cr→I	96.77	-	59.46
	I→Cr	90.43	0.0	56.21
DBA-O16	Cr→I	99.80	-	76.23
	I→Cr	92.73	0.0	73.43
DBA-O18	Cr→I	92.80	-	34.22
	I→Cr	83.10		37.09

where Cr=Crystal; N=Nematic ; I=Isotropic

4.3.3 Influence of Structural Changes (Alkyl chain) on Temperature Changes of DBA-On

A plot of the melting temperatures against the number of carbons in the alkoxy chain is shown in Figure 4.14. Based on the plot, it can be deduced that the mesophase behaviours are greatly influenced by the length of the terminal chain.

The plot shows a growing trend from C6 to C8 at beginning of the plot except for C10 which shows a fall off. In fact, as the chain length increases, the molecules become more flexible and disorder in going from the presumed all *trans* configuration in highly ordered crystalline state to more disorder mesophase or liquid phase (Kumar, 2001). Such flexibility will reduce the melting point. However, the melting temperatures exhibit ascending trend as the length of the terminal alkoxy chain of the derivatives increase from C12 to C16. This phenomenon can be attributed to the increase in the intermolecular Van der Waals attraction as the length of the alkoxy chain increased (Singh, 2001).

A decrease in the melting point is then observed when proceeding from the C16 derivative to the derivative with the longest terminal chain, C18. This is resulting from the dilution of its core system which induced by the increasing length of the alkyl chain.

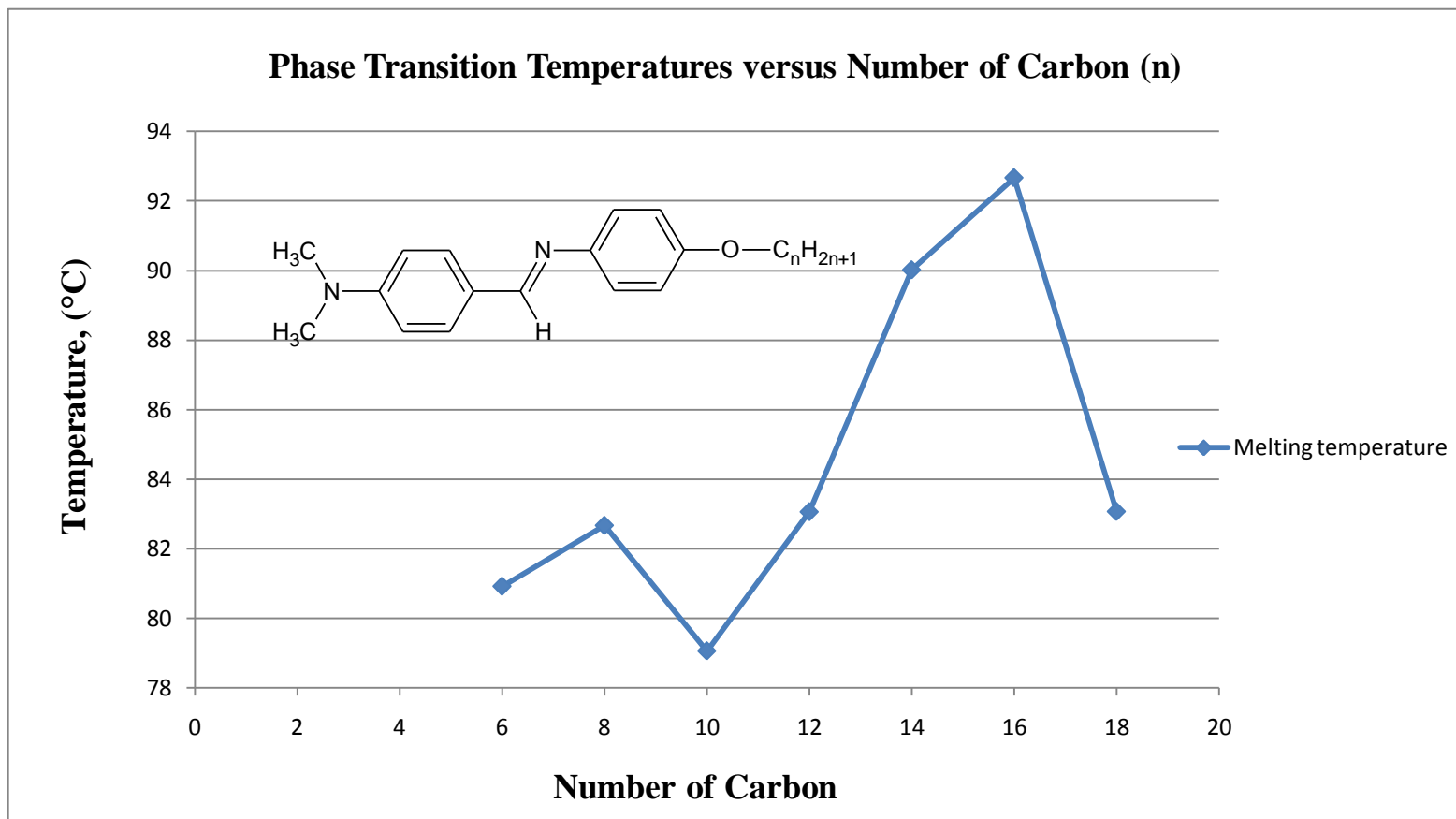


Figure 4.14: Plot of phase transition temperatures against number of carbon atom (n) in alkyloxy chain during heating scan

4.4 Structure Comparison with Related Compounds

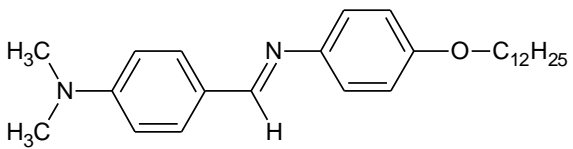
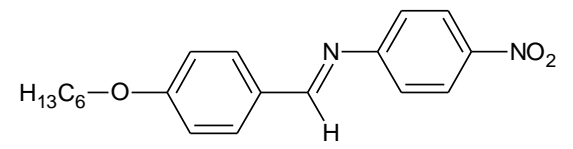
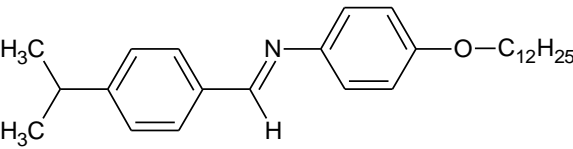
In the present work (**DBA-On**), the influence of the dimethylamino group is compared to other terminal substituents. The compounds of interest and their liquid crystalline data are tabulated in Table 4.8.

The physical properties of nematic mesogens are strongly influenced when a terminal group is attached to a nematic core (Singh, 2001). An attachment of a bulky terminal group will cause the core to be widened and increase the intermolecular separation. Therefore, the nematic phase stability is decreased due to the reduction in the lateral interactions. Terminally substituted compounds are found to exhibit more stable mesophase as compared to unsubstituted mesogenic compounds. Besides, the polarity of a terminal group tends to influence the formation of mesophase.

For the compound of **DBA-O12**, the polar dimethylamino group enhances the molecule's polarizability and intermolecular interactions which leads to the formation of the nematic phase. The strong electronegativity of N atom induced a strong terminal intermolecular interaction and enhances the formation of nematic phase. **DBA-O12** shows a monotropic nematic phase over the temperature ranges from 89.6 to 94.6 °C. The polar nitro group in compound **A** enhances the formation of monotropic nematic phase as well. The commencement of the nematic phase is from 75.6 to 79.5 °C. Despite the broadening effect, the less

electronegative carbon in isopropyl group still has a greater lateral interaction. Hence, it prefers the lamellar arrangements of smectic phase, this can be supported by compound of **series 1**. The compound of **series 1** exhibits enantiotropic smectic A phase for *n*-octyloxy and *n*-dodecyloxy derivatives whereas *n*-decyloxy and *n*-tetradecyloxy derivatives exhibit smectic A phase. Lower homologues as well as higher homologues of the **series 1** are non-mesogenic. This phenomenon can be explained as the isopropyl terminal group disturbs the order when molecules do not have very long chain length.

Table 4.8 Comparison of liquid crystalline properties of DBA-O12 with A, Han *et al.* (2004) and Series 1, Vora *et al.* (2000)

Compound	Structure and phase transition (°C)
DBA-O12	 <p style="text-align: center;">Cr 94.6 N 89.6 I</p>
A	 <p style="text-align: center;">Cr 83.0 N 79.5 I</p>
Series 1	 <p style="text-align: center;">Cr 54.5 SmA 60.0 I</p>

CHAPTER 5

CONCLUSION

A series of calamitic liquid crystals, *p-n*-(Dimethylamino)benzylidene-*p*-alkyloxyanilines, **DBA-On**, where n= 6, 8, 10, 12, 14, 16 and 18 was synthesized successfully. The final compounds differed from each other by the length of terminal alkyl chain. The structure of the liquid crystalline compounds were postulated using FTIR, ¹H NMR and ¹³C NMR spectroscopy and electron-ionization mass spectrometry. The final compounds are listed as following:

- *p-n*-(Dimethylamino)benzylidene-*p*-hexanoyloxyaniline (**DBA-O6**)
- *p-n*-(Dimethylamino)benzylidene-*p*-octanoyloxyaniline (**DBA-O8**)
- *p-n*-(Dimethylamino)benzylidene-*p*-decanoyloxyaniline (**DBA-O10**)
- *p-n*-(Dimethylamino)benzylidene-*p*-dodecanoyloxyaniline (**DBA-O12**)
- *p-n*-(Dimethylamino)benzylidene-*p*-tetradecanoyloxyaniline (**DBA-O14**)
- *p-n*-(Dimethylamino)benzylidene-*p*-hexadecanoyloxyaniline (**DBA-O16**)
- *p-n*-(Dimethylamino)benzylidene-*p*-octadecanoyloxyaniline (**DBA-O18**)

The IR spectral analysis of **DBA-On** confirmed the presence of C-H, C=O, C-O, C=C, C-N and C=N functional group. For ¹H NMR analysis, **DBA-O16** was chosen as the representative for the series of **DBA-On**. The appearance of azomethine proton (CH=N) signal at the chemical shift value of 8.36 ppm indicates the complete reaction of imination process. Signal found at δ = 4.00 ppm

confirmed the presence of the hydrogen of ether. For ^{13}C NMR, **DBA-O16** was selected as the representative for the **DBA-On** series. Azomethine carbon, $\text{CH}=\text{N}$ which appears at the most downfield region, $\delta = 159.1$ ppm is assigned. The signal emerges at the middle of the region, $\delta = 68.2$ ppm shows the complete reaction of Williamson etherification between intermediate, **DBAP** and potassium hydroxide. Mass spectroscopic analysis has been carried out on the representative compound **DBA-O16**. The molecular ion peak is observed at $m/z = 464.4$ while the base peak is shown at $m/z = 239.1$ due to the elimination of alkyl chain.

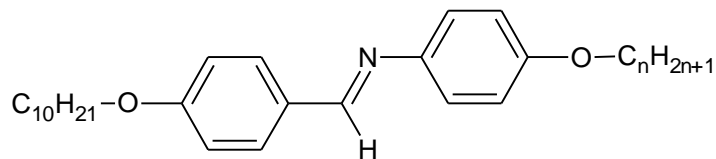
The liquid crystal properties are studied using POM. **DBA-O6** and **DBA-O12** are used as the representative compound in POM analysis. **DBA-O6** to **DBA-O12** exhibits monotropic behavior whereas **DBA-O14** to **DBA-O18** is non-mesogens. DSC technique is employed to obtain the transition temperature and associated enthalpy changes. **DBA-O12** shows monotropic behaviour whereby the liquid crystal phase is only observed during cooling cycle. The monotropic nematic phase is observed over relatively narrow temperature ranges from 89.59 to 96.86 °C. In the DSC thermogram, the molecular orientation is observed as below:

Crystal > Nematic > Isotropic
—————→
Increasing order

The mesophase behaviours are greatly influenced by the length of the terminal chain. As the length of the alkoxy chain increases, the increase in the intermolecular Van der Waals attraction leads to the increase of the melting point.

Future Study

Future study can be extended to the Schiff base compound with both alkyloxy groups as the terminal moiety especially those with longer chain. Both the ether group is attached on the para position of the Schiff base compound. Schiff base with the alkyloxy groups as the end group tend to generate different types of mesophases due to their rich polymorphism. In fact, the presence of nematic phase is mainly associated with the anisotropy shape while the presence of smectic phases depends on the polarity of a molecular structure. The moderate polar of ether group tends to enhance the molecular ordering and polarizability. This will then enhances the stability of smectic phase.



REFERENCES

Journal

- Galewaki, Z. and Coles, H. J. (1999). Liquid Crystalline Properties and Phase Situation in 4-chlorobenzylidene-4'-alkylanilines. *J. Mol. Liq.*, 79, 77-87.
- Godzwon, J., Sienkowska, M. J. and Galewski, Z. (2006). Smectic polymorphism of 4-decyloxybenzylidene-4'-alkyloxyanilines and their mixtures with polar standards of mesophases. *Phase Transitions*, 80, 217-229.
- Godzwon, J., Sienkowska, M. J. and Galewski, Z. (2007). Liquid crystalline properties of 4-hexyloxybenzylidene-4'-alkyloxyanilines. *Liq. Cryst.*, 34, 8, 911-917.
- Ha, S.T., Koh, T.M, Lin, H.C., Yeap, G. Y., Yip, F.W., Ong, S.T., Sivasothy, Y. and Ong, L.K. (2009). Heterocyclic benzothiazole-based liquid crystals: synthesis and mesomorphic properties. *Liq. Cryst.*, 36, 917-925.
- Ha, S.T., Ng, M.Y, Subramaniam, R.T., Ito, M.M., Saito, A., Watanabe, M., Lee, S.L and Bonde, N.L. (2010). Mesogenic azomethine esters with different end groups: Synthesis and thermotropic properties. *Int. J. Phys. Sci.*, 5(8), 1256-1262.
- Han, S.H., Yoshida, H., Nobe, Y., Fujiwara, M., Kamizori, J., Kikuchi, A., Iwahori, F. and Abe, J. (2005). Molecular alignment and thermal stability of liquid-crystalline phases in binary mixtures of electron donor and acceptor. *J. Mol. Struct.*, 735-736, 375-382

- J. S. Dave J.S. and Kurian G. (1977). Mesomorphic Behaviour of Schiff Base Esters-I: (a) p(p'-n-Alkoxybenzoyloxy)benzylidene-p'' -anisidines (b)p(p' - n-Alkoxybenzoyloxy)benzylidene-p'' -toluidines. *Mol. Cryst. Liq. Cryst.*, 42, 175-183.
- Kelker, H. and Scheurle, B. (1969). A Liquid Crystalline (Nematic) Phase with a Particularly Low Solidification Point. *Angew. Chem. Int. Edn.*, 8: 884- 885.
- Koleva, V., Dudev, T. and Wawer, I.(1997). ¹H and ¹³C NMR study and AM1 claculations of some azobenzenes and N-benzylideneanilines: effect of substituents on the molecular planarity. *J. Mol. Struct.*, 412, 153-159.
- Parra, M., Vergara, J., Alderete, J. and Zúrniga, C. (2004). Synthesis and mesomorphic properties of esters derived from Schiff's bases containing 1,3,4,-thiadiazole. *Liq. Cryst.*, 33, 11, 1531-1537.
- Prajapati, A.K., Vora, R.A. and Pandya. H.M. (2001). Effect of Lateral Hydroxy/ Alkoxy Group on Mesomorphism of Azobenzene Derivatives. *Mol. Cryst. Liq. Cryst.*, 369, 37-46.
- Prajapati, A.K., Thakkar, V. and Bonde, N. (2003). New Mesogenic Homologous Series of Schiff Base Cinnmates comprising Naphthalene Moiety. *Mol. Cryst. Liq. Cryst.*, 393, 41-48.
- Sitkowski, J., Stefaniak L., Dziembowska, T., Grech, E., Jagodzinska, E. and Webb, G.A. (1995). A multinuclear NMR study of proton transfer processes in Schiff bases. *J. Mol. Struct.*, 381, 177-180.
- Stability of Liquid Crystals Based on Different Central Linkages with Lateral Substitution and Terminal Heterocyclic Moieties. *Mol. Cryst. Liq. Cryst.*, 509, 173/[915]–185/[927].
- Thaker, B.T and Patel P. (2009). Synthesis, Mesophase Behavior and Thermal

Vora, R., Prajapati, A. and Kevat, J. (2000). Effects of terminal branching on mesomorphism. *Mol. Cryst. Liq. Cryst.*, 357, 229-237.

Vora, R.A. and Prajapati, A.K. (2001). New mesogenic homologous series of α -methylcinnamates. *Proc. Indian Acad. Sci. (Chem. Sci.)*, 113, 2, 2001, 95-102.

Yeap, G.Y., Ha, S.T., Boey, P.L., Ito, M.M., Sanehisa, S. and Youhei, Y. (2005). Synthesis, physical and mesomorphic properties of Schiff's base esters containing *ortho*-, *meta*-, *para*-substituents in benzylidene-4'-alkoxyanilines. *Mol. Cryst. Liq. Cryst.*, 33, 2, 205-211.

Yeap, G.Y., Ha, S.T., Boey, P.L., Mahmood, W.A.K., Ito, M.M. and Sanehisa, S. (2004), Synthesis and Mesomorphic Properties of Schiff Base esters *Ortho*-Hydroxy-*Para*-alkoxybenzylidene-*Para*-Substituted Anilines. *Mol. Cryst. Liq. Cryst.*, 423, 73-84.

Book chapter:

Carey, F.A., Sundberg, R.T. (2001). *Advanced Organic Chemistry, Part B: Reaction and Synthesis*, 4th Edition (pp166-167). New York. Kluwer Academic/Plenum Publishers.

Chandrasekhar, S. (1992). *Liquid Crystal*, 2nd Edition (pp 1-14). United Kingdom: Press Syndicate of the University of Cambridge.

Collings, P.J (2002). *Liquid crystal: nature's delicate phase of matter* (pp 131-163), 2nd edition. United Kingdom: Prinston and Oxford.

Collings, P.J and Hird, M. (1997). *Introduction to liquid crystals chemistry and physics* (pp 179-188), Taylor & Francis Ltd. London.

- Dierking, I. (2003). *Texture of liquid crystals* (pp 2-88), United Kingdom: Wiley-Vch Verlag.
- Hoffman, E and Stroobant V. (2005). *Mass spectroscopy principles and application* (pp172 -346), 2nd Edition. England. England: John Wiley & Sons Inc.
- Lam, C.K. (2007). *Liquid Crystal* (pp 1-11), 2nd Edition. United States of America: Wiley-interscience.
- Kumar, S. (2001), *Liquid Crystals: Experimental Study of Physical Properties and Phase Transitions* (pp 49-61, 397-451). United Kingdom: Cambridge University Press.
- Newham, R.E. (2005), *Properties of Materials, Anisotropy, Symmetry and Structure* (pp 333-336). New York.
- Pavia, D.L., Lampman, M.G. and Kriz, G.S. (2001). *Infrared spectroscopy. In Intoduciton to spectroscopy*, 3rd Edition. (pp 99-200). Washington: Brooks/ Cole.
- Silverstein, R.M. and Webster, F.X. (1998), *Spectrometric Identification of Organic Compounds* (pp 81-109), 6th Edition. Canada. John Wiley & Sons, Inc.
- Singh, S. (2001). *Liquid Crystal fundamental* (pp 15-232), 3rd Edition. New York: Plenum Press.
- Smart, L. and Gagan, M (2002), *The Molecular World: The Thrird Dimension* (pp 202 -208). United Kingdom. The Open University.
- Smith, B. (1999). *Infrared Spectral Interpretation: A Systematic Approach*. (pp 101). United States of America. CRC Press.

Smith, C.B (1996). *Fundamentals of fourier transform infrared spectroscopy* (pp 65-68). Florida: CRC Press LLC.

Smith, J.G. (2002). *Organic Chemistry* (pp 755, 803). New York. McGraw Hill.

Smith, M.B., March, J.(2000). *March's Advanced Organic Chemistry and Structures* (pp 486), 5th Edition. Canada. Wiley-Interscience Publication.

Solomons Graham, W.T. and Fryhle, C.B. (2000). *Organic chemistry*. (pp 477-497). United States of America: John Wiley & Sons Inc.

William H. Brown, Christopher S. Foote, Brent L. Iverson, Eric V. Anslyn (2009): *Organic chemistry* (pp 420-422), 5th edition. United States of America: Brooks/ Cole Cengage Learning.